
COMPARATIVE ANALYSIS OF WEATHER-BASED INDEXES AND THE ACTUARIES CLIMATE INDEX™ FOR CROP YIELD PREDICTION

A PREPRINT

✉ **Cem Yavrum**

Institute of Applied Mathematics
Middle East Technical University
06800, Ankara, Türkiye
cyavrum@metu.edu.tr

✉ **A. Sevtap Selcuk-Kestel**

Institute of Applied Mathematics
Middle East Technical University
06800, Ankara, Türkiye
skestel@metu.edu.tr

✉ **José Garrido**

Concordia University
Montreal, Canada
jose.garrido@concordia.ca

May 1, 2025

ABSTRACT

Climate change poses significant challenges to agriculture sector, affecting both crop productivity and economic stability. This study investigates the utility of climate indexes in predicting crop yields under diverse climatic conditions. Using generalized statistical models and machine learning algorithms, this research compares the predictive performance of long-established weather-based indexes with the Actuaries Climate Index™ (ACI), a newer entrant in the field, showcasing its potential for real-time applications and broader applicability across various sectors. To enhance model reliability and address multicollinearity among weather-related variables, the study incorporates both principal component analysis and functional principal component analysis. A total of 22 models, each constructed with different explanatory variables, highlight the significant impact of wind speed and sea-level changes alongside temperature and precipitation on crop yield variability. Furthermore, the ACI exhibits strong predictive capabilities, offering valuable insights for climate risk assessment and decision-making in agriculture and insurance-related sectors.

Keywords actuaries climate index · principal component analysis · crop yield · weather-based indexes · machine learning

1 Introduction

Climate change refers to long-term shifts in temperature and weather patterns, primarily driven by human-induced greenhouse gas emissions. Recent reports from the Intergovernmental Panel on Climate Change highlight the significant impact of human activities on global temperatures over the past few decades (IPCC 2022; Masson-Delmotte et al. 2021). One of the most concerning consequences of climate change is the increase in the frequency and intensity of heatwaves, which exacerbate heat-related illnesses and deaths. WHO (2014) projects that climate change could result in an additional 250,000 deaths annually between 2030 and 2050. Historical events underline the severity of this issue. For instance, in August 2003, France endured its hottest summer in 50 years, leading to over 14,000 fatalities (Kovats et al. 2004). Similarly, a 2010 heatwave in Quebec, Canada, caused a 33% spike in daily mortality rates and hospital emergency visits (Bustinza et al. 2013).

The financial risks for the insurance industry is heightened by climate change, primarily due to the increasing frequency and severity of extreme weather events such as hurricanes, floods, and wildfires. Gall et al. (2011) highlight that direct losses from natural hazards in the United States (U.S.) are steadily increasing and could reach \$300 to \$400 billion within a single decade. A specific example is the California wildfires of 2018, which Wang et al. (2021) estimated to have caused \$148.5 billion in damages, including capital losses, health costs, and indirect economic disruptions. More recently, the wildfires in the Los Angeles area have the potential to inflict up to \$250 billion in economic losses, making

them one of the most devastating natural disasters in U.S. history (Danielle 2025). From a broader perspective, Zhou et al. (2024) discuss the profound impact of climate change across various insurance sectors, including property/casualty, health, life, and crop insurance. They underscore the urgency for standardized methodologies to measure and quantify climate risks, ensuring that the industry can adapt to the sustainability challenges posed by a rapidly changing climate.

Climate change also leads to challenges like reduced crop yields and water scarcity, posing significant threats to global food security. Research by Lobell and Gourdji (2012) predicts that global warming could lower global crop yields by approximately 1.5% per decade, with potential reductions reaching as high as 4%. Several other studies reach similar results. For instance, Hu et al. (2024) observed that a 1°C rise in global temperatures results in a 6-8% average decrease in yields of major crops worldwide. Cai et al. (2009) project a 23-24% reduction in corn yields in central Illinois, U.S., by 2055, largely driven by increased water stress. Similarly, Adhikari et al. (2015) examine the impact of climate change on crops in Eastern Africa, concluding that the yields of major grains are significantly affected negatively, with wheat being particularly vulnerable—up to 72% of current yields are projected to decline.

Climate impact is mostly measured and interpreted by indexes. In the literature, various indexes such as the Climate Extremes Index (Karl et al. 1996), Greenhouse Climate Response Index (Karl et al. 1996), Palmer Drought Severity Index (Palmer 1965), Cooling Degree Days (Jewson and Brix 2005), Heating Degree Days (Jewson and Brix 2005) and Cumulative Rainfall Index (Odening et al. 2007) have been developed to quantify climate change, enabling researchers and policymakers to assess systematically its impact. These indexes often focus on critical variables such as temperature extremes, amounts of precipitation, drought severity, summarizing them into measurable indicators that facilitate the analysis of climate patterns and their consequences.

In recent years, the Actuaries Climate Index™ (ACI) has emerged as a pivotal tool for understanding and monitoring climate risks, offering valuable insights for insurance companies, governments, and the general public. Developed in 2016 by the four major North American actuarial societies, the ACI (2018) uses historical meteorological data from the United States and Canada to track extreme conditions in air temperature, precipitation, drought, wind, and sea-level rise. Its practical methodology has quickly been adapted for use in other countries. Curry (2015) demonstrates that the ACI methodology is applicable to regions like the United Kingdom and Europe, provided appropriate and sufficient meteorological data are available. The Australian Actuaries Climate Index (AACI 2018), which is tailored to Australian meteorological conditions, was introduced in 2018. The Turkish Actuaries Climate Index was developed in 2022 by Nevruz et al. (2022), and focuses on climate patterns specific to the Ankara region in Türkiye. Similarly, Zhou et al. (2023) launched the Iberian Actuarial Climate Index in 2023, marking the first application of the ACI framework to the European continent. It encompasses Spain and Portugal, offering localized insights into climate variability. Most recently, Garrido et al. (2023) adapt the ACI methodology to French data, creating the French Actuarial Climate Index. The continued adoption of the methodology worldwide demonstrates a growing global interest in effectively measuring and understanding climate risks.

This study aims to compare the Actuaries Climate Index™, with long-established weather-based indexes frequently used in energy and derivatives markets, by using regression models: generalized linear model (GLM) and generalized additive model (GAM), as well as machine learning algorithms: extreme gradient boosting (XGB) and light gradient boosting machine (LGBM). By evaluating these indexes based on their performance in predicting crop yields, a critical factor in the agricultural sector, the study demonstrates the robustness of the ACI, showcasing its potential for real-time applications and broader applicability across various sectors. Existing literature demonstrates the applicability of the ACI in various fields, particularly insurance and finance. Jiang and Weng (2019) analyze ACI's predictive power for stock returns of agriculture-related companies in the U.S. and Canada, concluding that ACI could support a profitable trading strategy. Pan et al. (2022) assess ACI's effectiveness in predicting corn yields in the Midwest region of the U.S. using linear and probit regression models, finding satisfactory predictive power. Zhou and Vilar-Zanón (2024) explore the relationship between the Spanish Actuarial Climate Index (SACI) and hailstorm-related losses in the wine grape insurance industry through linear and quantile regression models, noting a potential rise in monthly losses corresponding to future SACI increases.

Beyond comparing the predictive power of the indexes, this paper investigates the individual contribution of each weather index to model performance by fitting 22 distinct models, each constructed with different explanatory variables. This structured approach allows for a detailed assessment of how the inclusion of diverse weather indexes enhances the models' predictive accuracy and its explanatory power. Since all explanatory variables are weather-based, they may share common weather driven patterns, potentially leading to multicollinearity issues in regression models. Additionally, achieving comparable model performance with fewer explanatory variables is both practical and desirable. To address these challenges, dimension reduction techniques specifically, principal component analysis (PCA) and functional principal component analysis (FPCA) are applied to identify the most influential variables in the data sets. This approach not only mitigates multicollinearity issues but also simplifies the models, improving efficiency and interpretability.

The outcomes indicate that both ACI components and weather-based indexes exhibit robust predictive capabilities for crop yields (corn, wheat, soybeans) in the U.S. market. Furthermore, the findings reveal that incorporating indexes representing additional weather conditions—such as drought, wind, and sea-level—alongside traditional factors like air temperature and precipitation, substantially enhances model performance. This highlights the importance of a comprehensive approach that considers a broader spectrum of climatic variables to improve the accuracy and reliability of crop yield predictions.

The paper is organized as follows: Section 2 summarizes the climate indexes used in the study. Section 3 describes the proposed two-stage methodology and presents the framework of the 22 models developed for crop yield prediction. The properties of the data and the results of the analyses are provided in Section 4. Finally, Section 5 concludes the paper with a summary of the key findings and their implications. Additionally, regression models, machine learning algorithms and dimensionality reduction techniques used in the analyses are reviewed in the Appendix A.

2 Climate Indexes

We focus on weather-based indexes (WBI) such as Cooling Degree Day (CDD), Heating Degree Day (HDD) and Cumulative Rainfall Index (PRE), which are directly tied to temperature and rainfall. These indexes are particularly advantageous due to their reliance on single weather variables, making them simple to understand, straightforward to compute and convenient for comparative analysis with the Actuaries Climate Index™. Detailed formulations of these weather-based indexes and outlines of the corresponding components within the ACI framework are given below.

2.1 Weather-Based Indexes

CDD and HDD are temperature-based indexes, with CDD capturing warm weather conditions and HDD representing cool weather conditions. PRE, on the other hand, quantifies rainfall amounts. These indexes are initially calculated for daily time periods, and their values for longer intervals, such as monthly or meteorological seasons, are derived by summing the daily data. Briefly, CDD measures how much the outside air temperature exceeds a base level temperature (usually taken as 65°F or 18°C), and HDD measures the opposite, the temperature falls below a base level (Jewson and Brix 2005).

Let T_i^{\max} and T_i^{\min} denote the maximum and minimum temperatures measured on day i . The average temperature for day i is defined as,

$$T_i = \frac{T_i^{\max} + T_i^{\min}}{2}. \quad (1)$$

If the average temperature is higher than 65°F for CDD, and lower than 65°F for HDD, the difference becomes the CDD_i and HDD_i value for that day, respectively, given by,

$$CDD_i = \max\{T_i - 65, 0\}, \quad (2)$$

$$HDD_i = \max\{65 - T_i, 0\}. \quad (3)$$

On the other hand, PRE represents the total volume of rainfall accumulated over a specified time period (Odening et al. 2007), and is calculated by summing all daily rainfall measurements, expressed in millimeters, for the chosen time frame, such as a month or a meteorological season, described as

$$PRE = \sum_{t=1}^N r_t, \quad (4)$$

where r_t denotes the daily rainfall amount on day t , and N is the total number of days in the specified period.

2.2 Actuaries Climate Index™

The ACI is designed to improve understanding of climate trends and their potential impact, incorporating various climate variables that signify extreme weather conditions. It comprises six components: high temperature (T90), low temperature (T10), precipitation (P), drought (D), wind speed (W), and sea-level (S). Since each component reflects different weather conditions, the ACI uses standardized values for all components to integrate them into a single index.

Standardization is based on the mean and standard deviation of each component during the designated reference period of 1961 to 1990 (ACI 2018).

The components of the ACI used in our comparison analyses are briefly defined as follows:

- (i) T90 represents the percentage of days in a month when daily temperatures exceed the 90th percentile of the corresponding days in the reference period.
- (ii) T10 reflects the percentage of days when daily temperatures fall below the 10th percentile of the reference period.
- (iii) P, denoted as Rx5day, measures the maximum amount of rainfall recorded over any five consecutive days within a month.

The standardized values of each component are computed both on a monthly and seasonal basis. As described in Zhou et al. (2023), for each month (j) and year (k), these are:

$$T90_{STD}(j, k) = \frac{T90(j, k) - \mu_{T90(j)}}{\sigma_{T90(j)}}, \quad (5)$$

$$T10_{STD}(j, k) = \frac{T10(j, k) - \mu_{T10(j)}}{\sigma_{T10(j)}}, \quad (6)$$

$$P_{STD}(j, k) = \frac{Rx5day(j, k) - \mu_{Rx5day(j)}}{\sigma_{Rx5day(j)}}. \quad (7)$$

Here, $\mu_{(\cdot)}$ and $\sigma_{(\cdot)}$ are the mean and standard deviation of corresponding components for the reference period, respectively. The composite ACI is derived by averaging the standardized values of all six components, with the T10 component being assigned a negative value to account for its inverse relationship with warm weather conditions, and expressed as:

$$ACI = \frac{T90_{STD} - T10_{STD} + P_{STD} + D_{STD} + W_{STD} + S_{STD}}{6}. \quad (8)$$

Detailed information of ACI can be found in ACI (2018).

3 Methodology

The primary objective of this study is to assess the robustness of the ACI as a climate impact measure in the agriculture sector. Given that ACI is a relatively recent addition to the literature, its performance in predicting crop yields is compared with the performance of long-established weather-based indexes. By evaluating the predictive capabilities of climate indexes, the study seeks to demonstrate ACI's potential for real-time applications and its broader utility across various sectors.

The analyses are conducted in two stages. The first stage seeks similarities between WBI and ACI components. To do so, we first check how strongly correlated these two indexes are and define their empirical cumulative distribution functions. The assessment is conducted across three groups, each representing different weather conditions, enabling a systematic and detailed comparison of the two types of indexes, WBI and ACI. The second stage focuses on testing and comparing the predictive performance of climate indexes on crop yields. Crop yields are predicted by using regression models and machine learning algorithms that comprising a total of 22 distinct models, each constructed with different explanatory variables. This approach allows for a detailed analysis of the predictive performance of WBI and ACI, ensuring that variations in their predictive capabilities are systematically evaluated.

3.1 First Stage

Climate indexes that measure similar weather conditions are grouped into categories to facilitate meaningful comparisons. The grouping structure is based on the specific meteorological conditions represented by each index, such as warm weather, cool weather, and precipitation. Despite differences in their calculation methods, CDD defined in equation 2 and T90 in 5 measure warm weather conditions, HDD in 3 and T10 in 6 capture cool weather conditions, and PRE in 4

Table 1: Structure of groups

Group	Weather-Based Indexes (WBI)	Components of the ACI	Meteorological Season	Measurement
1	CDD	T90	Summer	Warm weather
2	HDD	T10	Winter	Cool weather
3	PRE	P	Spring	Precipitation

and P in 7 represent precipitation severity. This grouping ensures a systematic and logical comparison between the indexes, and its structure is summarized in Table 1.

For the comparisons, meteorological seasonal values (three months ending February, May, August, November) are used instead of monthly values. This approach aligns with the practical applications of climate indexes. For instance, CDD is commonly used to estimate energy demand during summer months, particularly for cooling, while HDD is used to evaluate heating needs during winter months (Spinoni et al. 2018). Regarding precipitation, its timing plays a critical role in agricultural productivity. Wang et al. (2016) highlight that wheat yields are especially sensitive to rainfall during the rainy season, while Peltonen-Sainio et al. (2011) point out that precipitation before harvest often negatively impacts crop yields. Therefore, in the precipitation group, index comparisons are performed for the spring months to encompass the rainy season preceding the general harvest period, which typically occurs during the summer months for most crops.

The dependence between the indexes are analyzed using the Spearman rank correlation coefficient (Zar 2005), a non-parametric measure that evaluates the strength and direction of the monotonic relationship between two variables. Distribution comparisons are performed using the Kolmogorov-Smirnov (K-S) test (Massey Jr 1951), which evaluates the maximum difference between the empirical cumulative distribution function values of the two data sets.

3.2 Second Stage

The predictive capabilities of climate indexes on the yields of corn (grain), wheat (winter), and soybeans are examined using both traditional statistical approaches and modern machine learning algorithms. In the literature, regression models (Ansarifar et al. 2021; Shah et al. 2018; Shastry et al. 2017) and machine learning techniques (Iniyan et al. 2023; Mahesh and Soundrapandiyan 2024; Nigam et al. 2019; Van Klompenburg et al. 2020) are frequently used for crop yield prediction, primarily due to their simplicity, interpretability, and computational efficiency. In this study, we use GLM and GAM, which are favored for their flexibility regarding distributional assumptions (detailed in Appendix A.1). Furthermore, to demonstrate the advantages of machine learning algorithms over traditional methods, we incorporate two widely used gradient boosting algorithms, XGB and LGBM (detailed in Appendix A.2).

Crop yields are influenced not only by weather conditions during the harvest period but also by extreme weather events throughout the growing season. Such conditions, including temperature extremes and precipitation anomalies, can have significant cumulative effects on crop development and productivity. To capture the full spectrum of potential impacts, all seasonal values for each index are included in the data sets. Additionally, the harvest period of each crop is carefully considered when structuring the data sets. Since corn and soybeans are typically harvested in autumn months, while wheat is harvested in summer months, the seasonal climate indexes are aligned accordingly. For corn and soybeans, the data sets cover the period from winter to autumn, whereas for wheat, they span from autumn to summer for each year. This approach ensures that the data sets encompass the entire year leading up to each crop’s harvest period. The analyses fit a total of 22 models, each incorporating explanatory variables representing various weather measurements and their combinations. A detailed breakdown of each model and the associated data sets is presented in Table 2. Comprehensive information on the data sets, along with the crop yields fitted by each model, is provided in full in Section 4.

Table 2: Explanatory variables included in predicting crop yields

Model #	Explanatory Variables	Model #	Explanatory Variables	Model #	Explanatory Variables
1	CDD	8	T90	15	T90-T10-P-W
2	HDD	9	T10	16	T90-T10-P-D
3	PRE	10	P	17	T90-T10-P-S
4	CDD-HDD	11	T90-T10	18	T90-T10-P-W-D
5	CDD-PRE	12	T90-P	19	T90-T10-P-W-S
6	HDD-PRE	13	T10-P	20	T90-T10-P-D-S
7	CDD-HDD-PRE	14	T90-T10-P	21	T90-T10-P-W-D-S
				22	ACI

Note. Based on four meteorological season values for each index.

The choice of explanatory variables for each model follows a logical progression, designed to evaluate the predictive power of various index configurations on crop yields. The first seven models are composed of WBI components and their combinations. The next set of seven models (Models 8–14) features indexes based on ACI components that correspond on a one-to-one basis with WBI variables. Additional ACI components (W, D, S) that are not represented in the initial 14 models are incorporated into the third set of seven models (Models 15–21). Lastly, the final one (Model 22) uses the composite ACI, which aggregates all six components into a single index, offering a comprehensive view of climate conditions in a composite measure.

A flowchart of the proposed methodology is illustrated in Figure 1. The methodology includes two distinct comparison frameworks to evaluate model performances based on different input variables. In the first comparison analysis, the performance of regression models and machine learning algorithms is assessed using principal components derived from the explanatory variables. Since all indexes incorporated into each model are weather-based, they tend to reflect similar meteorological patterns, which may result in multicollinearity issues in regression analyses. To ensure independence between the explanatory variables, and simplify the explanatory data sets without compromising model accuracy, we use PCA and FPCA (see details in Appendix A.3) as dimensionality reduction techniques. By comparing these two techniques, this study also evaluates the performance of FPCA relative to PCA in modeling time-dependent data like climate indexes.

Unlike regression models, machine learning algorithms do not require data simplification or the elimination of multicollinearity among variables. Therefore, in the second comparison analysis, the climate indexes are directly used as input variables in the machine learning algorithms without applying any dimensionality reduction. This approach not only allows for a direct assessment of model performance using the raw climate data but also provides a basis for evaluating the effectiveness of the principal component approach proposed in the methodology.

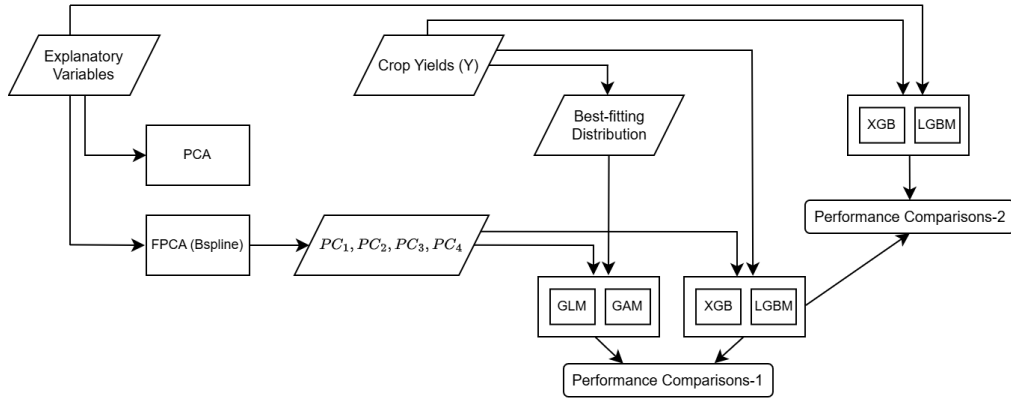


Figure 1: Flowchart of the proposed methodology

The “scikit-learn” (Fabian 2011) and “scikit-fda” (Ramos-Carreño et al. 2024) Python libraries are used to implement PCA and FPCA with a B-spline basis, respectively. To maintain consistency and simplicity in model execution, the default settings of both packages are applied. From the transformed data sets, the first four principal components (PC_1 , PC_2 , PC_3 , PC_4), which collectively account for more than 85% of the variance in the data, are selected as the input variables for analyses. This selection ensures that the models capture the majority of the information while reducing dimensionality.

Before conducting the regression analyses, the next critical step involves determining the appropriate link function of GLMs and GAMs, as well as the distribution of crop yield data. The Python package “distfit” (Taskesen 2020) is used to identify the most suitable distribution. This package evaluates 89 univariate distributions and selects the best-fitting one by comparing their residual sum of squares. To ensure consistency across GLMs and GAMs, the log-link function is applied in all models. This function is particularly well-suited for crop yield data, as these values are inherently positive and continuous. The implementation of GLMs and GAMs is carried out using the R packages “stats” (Team 2022) and “mgcv” (Wood 2015), respectively. The GLM used in the analyses is expressed as

$$\log(E(Y|PC_1, PC_2, PC_3, PC_4)) = \beta_0 + \sum_{i=1}^4 \beta_i * PC_i, \quad (9)$$

whereas the GAM is as follows

$$\log(E(Y|PC_1, PC_2, PC_3, PC_4)) = \beta_0 + \sum_{i=1}^4 f_i(PC_i). \quad (10)$$

Here, Y represents the crop yield data, PC_i ($i = 1, 2, 3, 4$) denote the principal components obtained through FPCA. β_i 's are the parameters, and $f_i(\cdot)$ are smooth functions capturing the potentially nonlinear relationships between principle components and the crop yields. In the analyses, Y and PC_i are included as vectors of size $n \times 1$ where n represents the number of observations (years).

For the construction of XGB and LGBM models, the Python packages “xgboost” (Brownlee 2019) and “lightgbm” (Microsoft 2017) are chosen among the alternatives, respectively. To maintain consistency, the same hyper-parameters are used in all models. These are the number of estimators (500), maximum depth (2), and learning rate (0.01). Model performance is assessed using two key metrics: the Pseudo- R^2 coefficient of determination (pR^2), and the Mean Absolute Percentage Error (MAPE). These metrics provide insights into both the explanatory power and prediction accuracy of the models.

4 Empirical Analysis

4.1 Data

Each component of the ACI consists of a time series, either on a monthly basis, or for meteorological seasons (three months ending February, May, August, November). These time series, starting in 1961, are derived from measurements collected at meteorological stations across the U.S. and Canada. The data are constructed separately for each country, in combination, and across 12 sub-regions. For consistency, this study uses U.S. data, where states are grouped into seven sub-regions based on their geographic locations: Alaska (ALA), Central East Atlantic (CEA), Central West Pacific (CWP), Midwest (MID), Southeast Atlantic (SEA), Southern Plains (SPL), and Southwest Pacific (SWP). The analyses use standardized seasonal values for each of the six ACI components (T90, T10, P, D, W, S) as well as the composite index (ACI). These seasonal data, obtained from the official Actuaries Climate Index™ website (<https://actuariesclimateindex.org/data/>, last accessed on April 18, 2025), cover a 63-year period from 1961 to 2023 for all seven sub-regions.

Regarding weather-based indexes, the National Oceanic and Atmospheric Administration (<https://www.ncei.noaa.gov/access/monitoring/products/>, last accessed on April 18, 2025) provides monthly data on CDD, HDD, and PRE for all U.S. states, covering the period from 1895 to the present. To align with the ACI data, seasonal values for CDD, HDD, and PRE between 1961 and 2023 are calculated by summing the monthly values for each meteorological season. Sub-regional data is subsequently generated by averaging the seasonal values of all states within each region. However, due to the unavailability of CDD and HDD data for Alaska, the analyses are limited to the six remaining regions of the U.S.

Annual crop yield data (in bushels per acre) for three major agricultural products-corn (grain), wheat (winter), and soybeans-produced in the U.S. is obtained from the United States Department of Agriculture (<https://quickstats.nass.usda.gov/>, last accessed on April 18, 2025) for all states, covering the period from 1961 to 2023. Following the same approach used in regional weather-based index calculations, sub-regional crop yields are calculated by averaging the annual yields of the states within each region. Analyses for corn and wheat are conducted across all regions, while for soybeans, due to data limitations, the analyses are restricted to four regions: CEA, CWP, MID, and SEA.

4.2 Results

The analyses start with determining the dependence among three groups (Table 1). It is noticed that all correlation coefficients, r , are statistically significant (p -value < 0.01), as shown in Table 3. Despite methodological differences in constructing the indexes, strong positive correlations are observed between the weather-based indexes and their corresponding components of the ACI. To assess the similarity of the distributions, we run K-S test which evaluates the null hypothesis that the distributions are identical. Table 3 also presents the indexes that exhibit statistically similar distributions, as indicated by p -values greater than 0.05. The results reveal that the precipitation-related indexes in Group-3 exhibit similar distributions across most regions compared to temperature measurements analyzed in the first two groups. Detailed descriptive statistics for each group are provided in Table B1 of the Appendix. Additionally, the indexes and their corresponding cumulative distribution function (CDF) values are illustrated in Figures B1 and B2 of the Appendix.

Table 3: Similarity tests within each group

		Region					
		CEA	CWP	MID	SEA	SPL	SWP
Group-1 (CDD-T90)	r	0.88	0.90	0.89	0.94	0.86	0.96
	K-S test (p)	0.089	<0.01	<0.01	<0.01	<0.01	0.408
Group-2 (HDD-T10)	r	0.89	0.83	0.86	0.87	0.81	0.79
	K-S test (p)	0.011	<0.01	<0.01	0.019	0.204	0.055
Group-3 (PRE-P)	r	0.83	0.81	0.87	0.87	0.68	0.85
	K-S test (p)	0.293	0.293	0.408	0.089	<0.01	0.089

Note. r: Spearman rank correlation coefficient.

In the second stage of the analysis, explanatory variables in each model are transformed into their principal components using PCA and FPCA. Figure 2 displays the total variation in the data sets, represented as regional averages, explained by the first four principal components derived from both methods for each model. The results demonstrate that the total variance explained by FPCA consistently surpasses that of PCA across all models, highlighting FPCA's superior performance when dealing with time-dependent data sets like climate indexes.

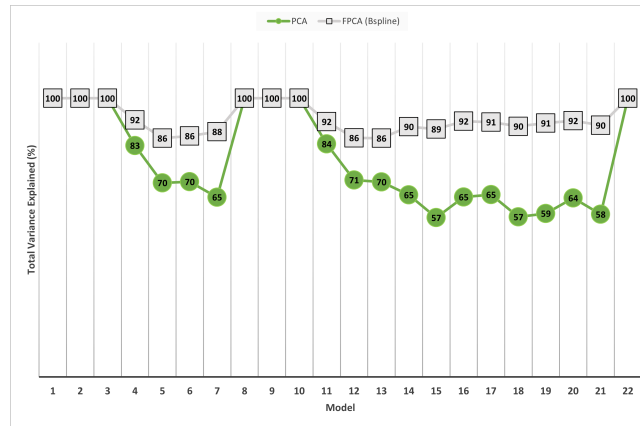


Figure 2: Explained variance comparisons of PCA and FPCA as regional averages

Upon closer examination of Figure 2, the models (1, 2, 3, 8, 9, 10, and 22) show a total explained variance of 100% for both PCA and FPCA. This is expected, as these models contain only one explanatory variable represented by its four seasonal values. Consequently, PCA and FPCA serve purely as data transformation tools for these cases without affecting the total variance explained.

For a detailed comparison of ACI components and their WBI counterparts, it is important to recall the structure of models outlined in Table 2. The first seven models are based on WBI components, while the subsequent seven models (Models 8–14) use their ACI counterparts. Comparing the total explained variance for paired models (e.g., 1 vs. 8, 2 vs. 9, 3 vs. 10, and so forth), it is clear that these values are nearly equivalent. For instance, the total variance explained by PCA for Model 4 is 83%, whereas it is 84% for Model 11. Similarly, FPCA explains 88% of the variance for Model 7 and 90% for Model 14. Since the choice of explanatory variables directly influence regression outcomes, ensuring high and comparable explained variance values across both index groups is crucial. Given that FPCA consistently explains a higher proportion of variance across all models, with values exceeding 85%, the principal components derived from FPCA are selected for the subsequent analyses, ensuring better model accuracy and reliability.

The distributions from the exponential family that best fit each crop yield for each region are identified, and the results are presented in Table 4. These distributions form the basis for estimating crop yields using GLMs and GAMs. Moreover, the incorporation of region-specific distributions ensures that the regression models account for spatial variability in crop yields, further improving the precision and relevance of the analyses.

Before proceeding with the analyses, the principal components derived from FPCA and the crop yields are divided into training and testing sets. Given the time series nature of the climate indexes, the first 57 years of the total 63-year period are allocated for training, while the remaining 6 years are used for testing, which corresponds to 90%-10% share. The models are fitted using training sets and their performance are measured by pR^2 . Tables 5 - 7 present the pR^2 values as regional averages for each crop, providing an overview of the models' explanatory power. To assess predictive accuracy on the test data, the MAPE is calculated and reported as regional averages in Figures 3 - 5. For a more detailed perspective, individual regional performance metrics are given in Tables B2–B9 of the Appendix.

Table 4: Best-fitting distributions for each crop

Region	Crop		
	Corn (Grain)	Wheat (Winter)	Soybeans
CEA	gamma	gamma	gamma
CWP	normal	normal	-
MID	normal	gamma	normal
SEA	gamma	gamma	gamma
SPL	normal	normal	gamma
SWP	normal	normal	-

A joint examination of Tables 5, 6, and 7 reveals that, for each crop and across all models, GAM consistently yields higher pR^2 than GLM, XGB outperforms LGBM, and ultimately, XGB achieves the highest pR^2 among all methods. However, this hierarchical performance pattern does not hold for MAPE values. For corn (Table 5 and Figure 3), Model 19 with XGB achieves the best performance with a pR^2 of 86.6% and a MAPE of 14.3%. The results of each model facilitate a detailed examination of the effects of individual components on crop yields. For instance, Model 14 (XGB), which includes temperature and precipitation components (T90, T10, P), achieves a pR^2 of 80.6% and a MAPE of 24.3%. Sequentially adding the wind (W), drought (D), and sea-level (S) components in Models 15, 16, and 17 allows for the evaluation of their individual impacts on performance. Among these 3 models, Model 17 (XGB) gives the best result with pR^2 of 85.8% and MAPE of 14.6%. The outcomes show that among the wind, drought and sea-level components, the component with the most pronounced positive impact on corn yield prediction is the sea-level (increasing the pR^2 from 80.6% to 85.8% and reducing the MAPE value from 24.3% to 14.5%). Furthermore, when the components of wind and sea-level are evaluated together (Model 19 with XGB), model success improves further, reaching a pR^2 of 86.6%, and a MAPE of 14.3%. Interestingly, Model 21, which incorporates all components of the ACI, exhibits worse performance compared to Model 19. This outcome suggests that, in addition to the positive contributions of wind and sea-level, the inclusion of the drought component has a diminishing effect on model performance when all other 5 climate variables of ACI are already used as predictors.

Table 5: pR^2 values (Train) of each model as regional averages, Corn (Grain)

Method	Model										
	1	2	3	4	5	6	7	8	9	10	11
GLM	0.288	0.296	0.170	0.286	0.334	0.353	0.384	0.217	0.231	0.292	0.248
GAM	0.384	0.388	0.309	0.396	0.475	0.414	0.444	0.389	0.446	0.416	0.381
XGB	0.738	0.747	0.691	0.753	0.757	0.766	0.769	0.690	0.732	0.734	0.708
LGBM	0.327	0.309	0.219	0.352	0.349	0.406	0.416	0.263	0.329	0.339	0.315
	12	13	14	15	16	17	18	19	20	21	22
GLM	0.372	0.391	0.406	0.392	0.378	0.574	0.420	0.584	0.551	0.515	0.403
GAM	0.481	0.553	0.454	0.457	0.533	0.644	0.469	0.689	0.677	0.625	0.516
XGB	0.775	0.797	0.806	0.780	0.790	0.858	0.790	0.866	0.864	0.856	0.788
LGBM	0.437	0.456	0.427	0.401	0.429	0.571	0.414	0.616	0.581	0.523	0.406

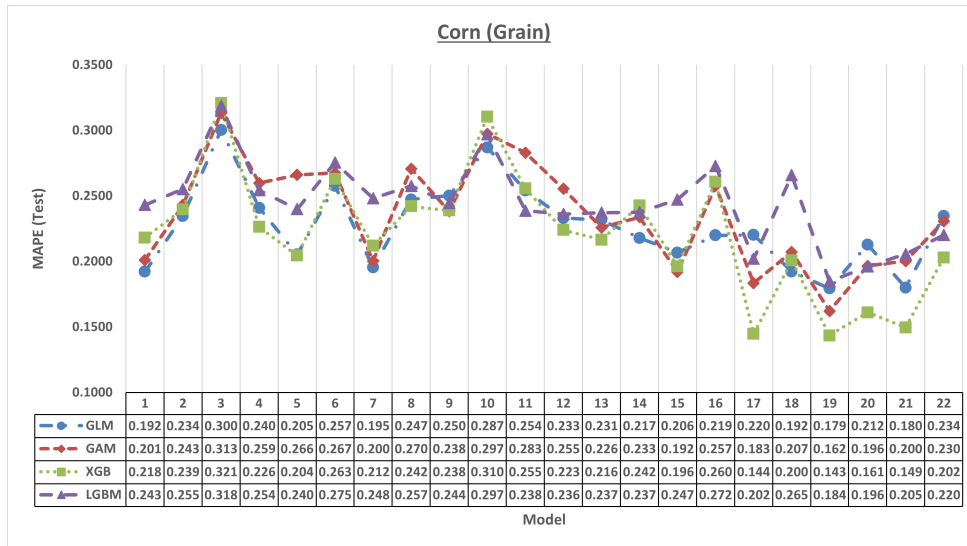


Figure 3: MAPE values (Test) of each model as regional averages, Corn (Grain)

For wheat (Table 6 and Figure 4), as with corn, Model 19 yields the best overall performance. However, GAM outperforms XGB, particularly with respect to MAPE values. While XGB consistently achieves a better fit to the training data across all models, this does not correspond to better predictive performance on the test data. For instance, GAM records a lower MAPE of 12.4% with a pR^2 of 61.9%, whereas XGB attains a higher pR^2 of 84.2% but with a higher MAPE of 14.6%. On the other hand, the pR^2 values obtained with GAM for Model 8 (T90), Model 9 (T10), and Model 10 (P) are 39.8%, 43.6%, and 39.7%, respectively. These results suggest that, when assessed individually, precipitation has a relatively smaller impact on wheat yield prediction compared to the temperature-related components. However, when precipitation is combined with low-temperature extremes (as in Model 13), model performance improves significantly, with the pR^2 increasing to 52.9%.

Table 6: pR^2 values (Train) of each model as regional averages, Wheat (Winter)

Method	Model										
	1	2	3	4	5	6	7	8	9	10	11
GLM	0.262	0.296	0.118	0.301	0.282	0.345	0.333	0.215	0.260	0.239	0.242
GAM	0.439	0.515	0.360	0.527	0.372	0.400	0.433	0.398	0.436	0.397	0.359
XGB	0.725	0.756	0.659	0.752	0.730	0.737	0.776	0.725	0.738	0.696	0.723
LGBM	0.289	0.353	0.162	0.346	0.300	0.321	0.320	0.328	0.318	0.260	0.288
	12	13	14	15	16	17	18	19	20	21	22
GLM	0.360	0.349	0.355	0.397	0.333	0.526	0.366	0.552	0.532	0.494	0.439
GAM	0.493	0.529	0.458	0.516	0.483	0.599	0.439	0.619	0.593	0.538	0.535
XGB	0.781	0.741	0.747	0.786	0.765	0.842	0.786	0.842	0.841	0.825	0.788
LGBM	0.367	0.371	0.327	0.417	0.362	0.524	0.408	0.552	0.538	0.507	0.440

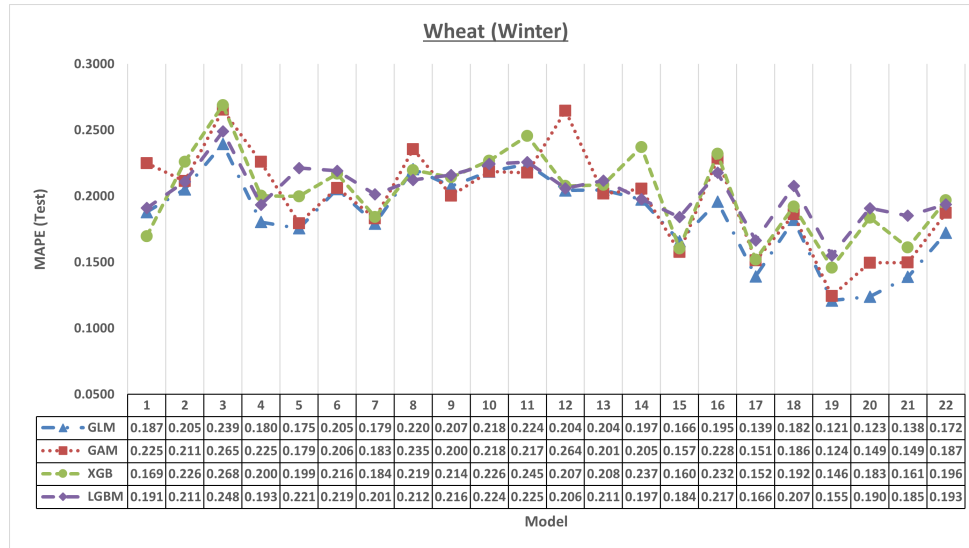


Figure 4: MAPE values (Test) of each model as regional averages, Wheat (Winter)

For soybeans, the findings diverge slightly from those for corn and wheat. As shown in Table 7 and Figure 5, the best model is Model 17 with GAM, which achieves a pR^2 of 72.1% and a MAPE of 12.56%. Notably, the inclusion of the wind component in the models appears to negatively affect the performance for soybean yield, in contrast to its role in models for corn and wheat. When examining the impact of individual components, the performance difference between Models 12 (T90 and P) and Model 13 (T10 and P) is noteworthy. For instance, Model 12 with XGB achieves a pR^2 of 74%, and a MAPE of 24.9% whereas Model 13 achieves a higher pR^2 of 78.6%, and a lower MAPE value of 20.5%. This indicates that cold weather extremes (T10) exert a stronger influence on soybean yield compared to warm weather extremes (T90). This conclusion is further supported by the performance results of Model 8 (only T90, pR^2 : 66.6%, MAPE: 27.3%) and Model 9 (only T10, pR^2 : 72.7%, MAPE: 25.8%).

When analyzing the best-performing models for the three crops (Model 19 for corn and wheat, Model 17 for soybeans), it becomes clear that, in addition to temperature and precipitation variables, sea-level change plays a significant role in predicting yields. One possible explanation for this is that variations in sea-level can impact crop production more broadly, particularly through mechanisms such as increased soil salinity, flooding, and the loss of agricultural land. Furthermore, wind appears to have a less pronounced effect on soybean yield compared to corn and wheat. This could be attributed to the relatively short stature of soybean plants, making them more resistant to wind-induced damage. In

Table 7: pR^2 values (Train) of each model as regional averages, Soybeans

Method	Model										
	1	2	3	4	5	6	7	8	9	10	11
GLM	0.250	0.265	0.254	0.234	0.377	0.387	0.442	0.128	0.182	0.319	0.164
GAM	0.327	0.350	0.421	0.352	0.491	0.426	0.534	0.302	0.515	0.431	0.318
XGB	0.675	0.723	0.706	0.689	0.774	0.773	0.784	0.666	0.727	0.732	0.663
LGBM	0.222	0.252	0.258	0.286	0.357	0.426	0.425	0.146	0.314	0.326	0.235
	12	13	14	15	16	17	18	19	20	21	22
GLM	0.341	0.378	0.402	0.362	0.389	0.602	0.374	0.597	0.573	0.567	0.381
GAM	0.467	0.571	0.479	0.441	0.615	0.721	0.422	0.641	0.695	0.606	0.528
XGB	0.740	0.786	0.761	0.770	0.768	0.862	0.752	0.861	0.847	0.838	0.756
LGBM	0.367	0.436	0.354	0.368	0.387	0.558	0.348	0.537	0.510	0.526	0.343

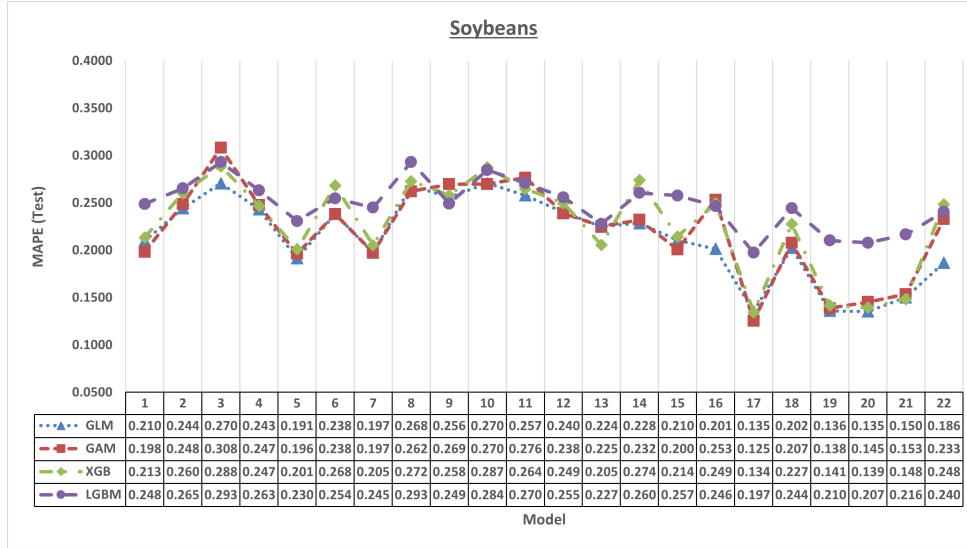


Figure 5: MAPE values (Test) of each model as regional averages, Soybeans

contrast, taller crops like corn and wheat may be more vulnerable to lodging¹ and other wind-related stresses, which can negatively impact their overall yield.

A detailed comparison of the predictive performance between ACI components and their WBI counterparts on crop yields reveals varying results depending on the methods for paired models (1 vs. 8, 2 vs. 9, 3 vs. 10, and so forth). While performance differences are more pronounced in the GAM results, the XGB results indicate minimal differences between the paired models. For instance, based on GAM results for corn (Table 5), the performance difference between Model 1 (CDD, pR^2 : 38.4%) and Model 8 (T90, pR^2 : 38.9%) is negligible at just 0.5%, suggesting comparable explanatory power between CDD and T90. However, a more substantial gap is observed between Model 3 (PRE, pR^2 : 30.9%) and Model 10 (P, pR^2 : 41.6%), amounting to 10.7%. A similar pattern emerges for wheat (Table 6), where the performance gap between Model 7 (pR^2 : 43.3%) and Model 14 (pR^2 : 45.8%) remains limited at 2.5%, but increases significantly to 16.8% between Model 4 (pR^2 : 52.7%) and Model 11 (pR^2 : 35.9%), highlighting a notable variation in the predictive value of the corresponding indexes. In contrast, XGB results across all paired models and crops demonstrate a maximum performance difference of only 5%, with an average of 2.5%, underscoring the overall similarity in the predictive effectiveness of ACI components and their WBI counterparts.

Another critical observation is that the final model (Model 22), which uses the composite ACI by aggregating all six components into a single index, consistently underperforms compared to Model 21, which incorporates each component separately, across all crops and methods. These findings highlight that the composite ACI index alone fails to fully capture and explain the complex weather conditions affecting crop yields. This suggests that treating the individual components separately provides a more nuanced and effective modeling approach, ensuring greater accuracy in predicting yield variations.

The second comparison analysis is designed to evaluate the performance sensitivity of machine learning algorithms with respect to different input variables. Table 8 presents only the results of XGB for the second comparison analysis, as it outperformed LGBM in earlier analyses. In Table 8, XGB refers to the results obtained using principal components

¹Lodging is the bending over of the stems of crops which makes them very difficult to harvest. It usually happens due to the wind-related stress.

derived from climate indexes, while XGB-C corresponds to the scenario where the climate indexes are directly used as input variables. Notably, with the XGB-C method, Model 21 (which incorporates all six components of ACI and thus constitutes the largest data set) consistently yields the best performance, with only a slight difference compared to the second-best models. Among the remaining models that exclude one or more components, the second-best performing models remain consistent with those from the first comparison analysis (Model 19 for corn and wheat, Model 17 for soybeans). One possible explanation for this is that the direct use of climate indexes preserves all original information in the data sets, enabling machine learning algorithms to process and use a greater number of features more effectively, compared to the more compressed data sets derived through principal component analysis. Regional performance metrics of XGB-C are given in Tables B10–B11 of the Appendix.

It is also noteworthy that across all analyses, the best-performing models for each crop remain consistent across all methods (GLM, GAM, XGB, LGBM). This consistency underscores the substantial impact of specific climate indexes on crop yields, demonstrating that their predictive value holds true regardless of the modeling approach.

Table 8: Performance Comparison-2 as regional averages for each crop

Model	Corn (Grain)				Wheat (Winter)				Soybeans			
	pR2 (Train)		MAPE (Test)		pR2 (Train)		MAPE (Test)		pR2 (Train)		MAPE (Test)	
	XGB	XGB-C	XGB	XGB-C	XGB	XGB-C	XGB	XGB-C	XGB	XGB-C	XGB	XGB-C
1	0.738	0.741	0.218	0.199	0.725	0.704	0.170	0.166	0.675	0.713	0.213	0.226
2	0.747	0.723	0.240	0.243	0.756	0.746	0.226	0.197	0.723	0.703	0.260	0.276
3	0.691	0.663	0.321	0.323	0.659	0.660	0.269	0.267	0.706	0.723	0.289	0.285
4	0.753	0.822	0.226	0.221	0.752	0.814	0.200	0.187	0.689	0.819	0.247	0.264
5	0.757	0.848	0.204	0.207	0.730	0.822	0.200	0.190	0.774	0.834	0.201	0.222
6	0.766	0.842	0.263	0.246	0.737	0.849	0.217	0.193	0.773	0.859	0.268	0.260
7	0.769	0.877	0.212	0.208	0.776	0.881	0.184	0.184	0.784	0.886	0.205	0.233
8	0.690	0.726	0.242	0.260	0.725	0.718	0.220	0.209	0.666	0.630	0.273	0.294
9	0.732	0.728	0.239	0.235	0.738	0.755	0.214	0.202	0.727	0.731	0.258	0.253
10	0.734	0.750	0.310	0.326	0.696	0.740	0.227	0.243	0.732	0.750	0.287	0.303
11	0.708	0.811	0.256	0.218	0.723	0.811	0.246	0.208	0.663	0.776	0.265	0.236
12	0.775	0.880	0.224	0.235	0.781	0.852	0.208	0.201	0.740	0.845	0.250	0.260
13	0.797	0.853	0.217	0.225	0.741	0.859	0.209	0.186	0.786	0.846	0.206	0.245
14	0.806	0.894	0.243	0.206	0.747	0.885	0.237	0.187	0.761	0.879	0.274	0.234
15	0.780	0.933	0.196	0.179	0.786	0.922	0.161	0.142	0.770	0.927	0.214	0.209
16	0.790	0.909	0.261	0.211	0.765	0.899	0.232	0.193	0.768	0.893	0.249	0.230
17	0.858	0.950	0.145	0.141	0.842	0.943	0.152	0.132	0.862*	0.957^φ	0.134*	0.134^φ
18	0.790	0.941	0.201	0.180	0.786	0.935	0.192	0.138	0.752	0.935	0.228	0.197
19	0.866*	0.963^φ	0.143*	0.136^φ	0.842*	0.954^φ	0.146*	0.124^φ	0.861	0.941	0.142	0.134
20	0.864	0.961	0.161	0.144	0.841	0.949	0.184	0.133	0.847	0.953	0.139	0.140
21	0.856	0.964*	0.150	0.135*	0.825	0.960*	0.161	0.119*	0.838	0.963*	0.148	0.130*
22	0.788	0.780	0.203	0.203	0.788	0.773	0.197	0.166	0.756	0.772	0.249	0.228

Note. * Best results, ^φ Second best results.

5 Concluding Remarks

This study examines the Actuaries Climate Index™ within the agricultural sector and compares its effectiveness with widely recognized weather-based indexes. The focus is on evaluating the predictive capabilities of both ACI components and traditional weather-based indexes in predicting three selected crop yields. By fitting 22 distinct models, each constructed with different climate indexes and their combinations, this paper also investigates the individual contribution of each weather index to model performance. Based on high goodness-of-fit test results and low MAPE values, climate indexes exhibit strong predictive power in modelling crop yields. The key insights drawn from the analyses can be summarized as follows:

- (i) The FPCA consistently outperforms the traditional PCA in terms of explanatory variance, when applied to time-dependent climate indexes.
- (ii) The four principal components derived through FPCA are sufficiently effective in capturing the underlying patterns in crop yield variations.
- (iii) ACI components and their WBI counterparts exhibit strong correlation, and deliver similar predictive performance in predicting crop yields, especially with machine learning algorithms.
- (iv) The inclusion of indexes representing additional weather conditions—such as wind speed, and sea-level changes—alongside temperature and precipitation, significantly improves model performance.
- (v) The composite ACI index alone fails to fully capture and explain the complex weather conditions affecting crop yields.

The outcomes suggest that the ACI framework has a potential to serve as a valuable climate risk indicator not only for the agricultural sector but also for the finance and insurance industries, where climate-related metrics are becoming increasingly critical for risk assessment and decision-making.

Despite the promising performance metrics achieved, the study can be further improved in several aspects. One notable limitation is that regional crop yields were assessed by averaging the annual yields of the states within each region. This approach overlooks the fact that some states may have a greater influence on regional agricultural output due to their size or productivity levels. Moreover, the selection of the best-performing models for each crop is based on regional average results, which may not accurately reflect optimal performance at the regional level. Consequently, identifying and evaluating the best models for each specific region or state would enhance the precision and applicability of the findings, particularly for targeted applications in the insurance sector.

The proposed methodology also contributes to the literature on forecasting crop yields. Forecasting weather-related factors that significantly impact crop yields such as temperature, precipitation, and sea-level, often requires complex, time-consuming methods due to their inherently dynamic nature. However, by incorporating future projections of components derived through the FPCA method, crop yield forecasts can be achieved in a more efficient and convenient manner.

Acknowledgments

Jose Garrido gratefully acknowledges the financial support of the Natural Sciences and Engineering Research Council of Canada (RGPIN-2017-06643).

References

- AACI. *Design Documentation: Australian Actuaries Climate Index*. The Institute of Actuaries, Australia, 2018. Available online: <https://www.actuaries.asn.au/microsites/climate-index/about/development-and-design> (last accessed on 18 April 2025).
- ACI. *Actuaries Climate Index: Development and Design*. American Academy of Actuaries, the Canadian Institute of Actuaries, the Casualty Actuarial Society, and the Society of Actuaries, 2018. Available online: <https://actuariesclimateindex.org/wp-content/uploads/2019/05/ACI.DevDes.2.20.pdf> (last accessed on 18 April 2025).
- Umesh Adhikari, A Pouyan Nejadhashemi, and Sean A Woznicki. Climate change and eastern africa: a review of impact on major crops. *Food and energy security*, 4(2):110–132, 2015.
- Javad Ansarifar, Lizhi Wang, and Sotirios V Archontoulis. An interaction regression model for crop yield prediction. *Scientific reports*, 11(1):17754, 2021.
- Jason Brownlee. Xgboost with python. *Machine Learning Mastery*, 2019.
- Ray Bustinza, Germain Lebel, Pierre Gosselin, Diane Bélanger, and Fateh Chebana. Health impacts of the july 2010 heat wave in québec, canada. *BMC public health*, 13:1–7, 2013.
- Ximing Cai, Dingbao Wang, and Romain Laurent. Impact of climate change on crop yield: A case study of rainfed corn in central illinois. *Journal of Applied Meteorology and Climatology*, 48(9):1868–1881, 2009.
- Tianqi Chen and Carlos Guestrin. Xgboost: A scalable tree boosting system. In *Proceedings of the 22nd acm sigkdd international conference on knowledge discovery and data mining*, pages 785–794, 2016.
- C Curry. Extension of the actuaries climate index to the uk and europe. *A Feasibility Study. Institute and Faculty of Actuaries*, 2015.
- Monica Danielle. Accuweather estimates more than 250 billion (us dollar) in damages and economic loss from la wildfires, Jan 2025. URL <https://www.accuweather.com/en/weather-news/accuweather-estimates-more-than-250-billion-in-damages-and-economic-loss-from-la-wildfires/1733821>.
- Pedregosa Fabian. Scikit-learn: Machine learning in python. *Journal of machine learning research* 12, page 2825, 2011.
- Melanie Gall, Kevin A Borden, Christopher T Emrich, and Susan L Cutter. The unsustainable trend of natural hazard losses in the united states. *Sustainability*, 3(11):2157–2181, 2011.
- José Garrido, Xavier Milhau, and Anani Olympio. The definition of a french actuarial climate index; one more step towards a european index. 2023.
- Trevor J Hastie. Generalized additive models. *Statistical models in S*, pages 249–307, 2017.

- Harold Hotelling. Analysis of a complex of statistical variables into principal components. *Journal of educational psychology*, 24(6):417, 1933.
- Tongxi Hu, Xuesong Zhang, Sami Khanal, Robyn Wilson, Guoyong Leng, Elizabeth M Toman, Xuhui Wang, Yang Li, and Kaiguang Zhao. Climate change impacts on crop yields: A review of empirical findings, statistical crop models, and machine learning methods. *Environmental Modelling & Software*, page 106119, 2024.
- S Iniyan, V Akhil Varma, and Ch Teja Naidu. Crop yield prediction using machine learning techniques. *Advances in Engineering Software*, 175:103326, 2023.
- IPCC. *Climate Change 2022: Impacts, Adaptation, and Vulnerability*. Cambridge University Press, 2022. Available online: <https://www.ipcc.ch/report/sixth-assessment-report-working-group-ii/> (last accessed on 18 April 2025).
- Stephen Jewson and Anders Brix. *Weather derivative valuation: the meteorological, statistical, financial and mathematical foundations*. Cambridge University Press, 2005.
- Ruihong Jiang and Chengguo Weng. Climate change risk and agriculture-related stocks. Available at SSRN 3506311, 2019.
- Thomas R Karl, Richard W Knight, David R Easterling, and Robert G Quayle. Indices of climate change for the united states. *Bulletin of the American Meteorological Society*, 77(2):279–292, 1996.
- Guolin Ke, Qi Meng, Thomas Finley, Taifeng Wang, Wei Chen, Weidong Ma, Qiwei Ye, and Tie-Yan Liu. Lightgbm: A highly efficient gradient boosting decision tree. *Advances in neural information processing systems*, 30, 2017.
- Sari Kovats, Tanja Wolf, and Bettina Menne. Heatwave of august 2003 in europe: provisional estimates of the impact on mortality. *Weekly releases (1997–2007)*, 8(11):2409, 2004.
- David B Lobell and Sharon M Gourdj. The influence of climate change on global crop productivity. *Plant physiology*, 160(4):1686–1697, 2012.
- Pavithra Mahesh and Rajkumar Soundrapandiyam. Yield prediction for crops by gradient-based algorithms. *Plos one*, 19(8):e0291928, 2024.
- Frank J Massey Jr. The kolmogorov-smirnov test for goodness of fit. *Journal of the American statistical Association*, 46(253):68–78, 1951.
- Valérie Masson-Delmotte, Panmao Zhai, Anna Pirani, Sarah L Connors, Clotilde Péan, Sophie Berger, Nada Caud, Y Chen, L Goldfarb, MI Gomis, et al. Climate change 2021: the physical science basis. *Contribution of working group I to the sixth assessment report of the intergovernmental panel on climate change*, 2(1):2391, 2021.
- Microsoft. *LightGBM Python-package*, 2017. Available online: <https://github.com/microsoft/LightGBM/tree/master/python-package> (last accessed on 18 April 2025).
- John Ashworth Nelder and Robert WM Wedderburn. Generalized linear models. *Journal of the Royal Statistical Society Series A: Statistics in Society*, 135(3):370–384, 1972.
- Ezgi Nevruz, Raif Yakup Atıcı, and Kasirga Yildirak. Actuaries climate index: An application for turkey. *İstatistik Araştırma Dergisi*, 12(2):14–25, 2022.
- Aruvansh Nigam, Saksham Garg, Archit Agrawal, and Parul Agrawal. Crop yield prediction using machine learning algorithms. In *2019 fifth international conference on image information processing (ICIIP)*, pages 125–130. IEEE, 2019.
- Martin Odening, Oliver Mußhoff, and Wei Xu. Analysis of rainfall derivatives using daily precipitation models: Opportunities and pitfalls. *Agricultural Finance Review*, 67(1):135, 2007.
- Wayne C Palmer. Meteorological drought. us. *Weather Bureau Res. Paper*, 45:1–58, 1965.
- Qimeng Pan, Lysa Porth, and Hong Li. Assessing the effectiveness of the actuaries climate index for estimating the impact of extreme weather on crop yield and insurance applications. *Sustainability*, 14(11):6916, 2022.
- Karl Pearson. Liii. on lines and planes of closest fit to systems of points in space. *The London, Edinburgh, and Dublin philosophical magazine and journal of science*, 2(11):559–572, 1901.
- Pirjo Peltonen-Sainio, Lauri Jauhiainen, and Kaija Hakala. Crop responses to temperature and precipitation according to long-term multi-location trials at high-latitude conditions. *The Journal of Agricultural Science*, 149(1):49–62, 2011.
- Carlos Ramos-Carreño, José Luis Torrecilla, Miguel Carbajo-Berrocal, Pablo Marcos, and Alberto Suárez. scikit-fda: a python package for functional data analysis. *Journal of Statistical Software*, 109:1–37, 2024.
- James O Ramsay and Bernard W Silverman. *Applied functional data analysis: methods and case studies*. Springer, 2002.

- Ayush Shah, Akash Dubey, Vishesh Hemnani, Divye Gala, and DR Kalbande. Smart farming system: Crop yield prediction using regression techniques. In *Proceedings of International Conference on Wireless Communication: ICWiCom 2017*, pages 49–56. Springer, 2018.
- Han Lin Shang. A survey of functional principal component analysis. *AStA Advances in Statistical Analysis*, 98: 121–142, 2014.
- Aditya Shastry, HA Sanjay, and E Bhanusree. Prediction of crop yield using regression techniques. *International Journal of Soft Computing*, 12(2):96–102, 2017.
- Jonathan Spinoni, Jürgen V Vogt, Paulo Barbosa, Alessandro Dosio, Niall McCormick, Andrea Bigano, and Hans-Martin Füssel. Changes of heating and cooling degree-days in europe from 1981 to 2100. *Int. J. Climatol*, 38(51): e191–e208, 2018.
- Erdogan Taskesen. distfit is a python library for probability density fitting., Jan 2020. URL <https://erdogant.github.io/distfit>.
- R Development Core Team. R: A language and environment for statistical computing. 2022.
- Thomas Van Klompenburg, Ayalew Kassahun, and Cagatay Catal. Crop yield prediction using machine learning: A systematic literature review. *Computers and electronics in agriculture*, 177:105709, 2020.
- Daoping Wang, Dabo Guan, Shupeng Zhu, Michael Mac Kinnon, Guannan Geng, Qiang Zhang, Heran Zheng, Tianyang Lei, Shuai Shao, Peng Gong, et al. Economic footprint of california wildfires in 2018. *Nature Sustainability*, 4(3): 252–260, 2021.
- Xiaobin Wang, Dianxiong Cai, Huijun Wu, WB Hoogmoed, and O Oenema. Effects of variation in rainfall on rainfed crop yields and water use in dryland farming areas in china. *Arid Land Research and Management*, 30(1):1–24, 2016.
- WHO. Quantitative risk assessment of the effects of climate change on selected causes of death, 2030s and 2050s. In *Quantitative risk assessment of the effects of climate change on selected causes of death, 2030s and 2050s*. 2014.
- Simon Wood. Package ‘mgcv’. *R package version*, 1(29):729, 2015.
- Simon N Wood. *Generalized additive models: an introduction with R*. chapman and hall/CRC, 2017.
- Jerrold H Zar. Spearman rank correlation. *Encyclopedia of biostatistics*, 7, 2005.
- Nan Zhou and José L Vilar-Zanón. Impact assessment of climate change on hailstorm risk in spanish wine grape crop insurance: Insights from linear and quantile regressions. *Risks*, 12(2):20, 2024.
- Nan Zhou, José Luis Vilar-Zanón, José Garrido, and Antonio-José Heras Martínez. On the definition of an actuarial climate index for the iberian peninsula. In *Anales del Instituto de Actuarios Españoles*, number 29, pages 37–59, 2023.
- Nan Zhou, José Luis Vilar-Zanón, Jose Garrido, and Antonio José Heras-Martínez. Measuring climate change from an actuarial perspective: a survey of insurance applications. *Global Policy*, 15:34–46, 2024.

Appendix

A Preliminaries

In this section, we provide an overview of generalized linear models (GLMs) and generalized additive models (GAMs), which belong to the class of generalized statistical models, as well as Extreme Gradient Boosting (XGB) and Light Gradient Boosting Machine (LGBM), which are classified as machine learning algorithms. Furthermore, we review principal component analysis (PCA) and functional principal component analysis (FPCA), two dimensionality reduction techniques used to preprocess and simplify data sets before being incorporated into the models.

A.1 Generalized Statistical Models

GLMs are widely used regression framework that extends traditional linear models by accommodating response variables with error distributions other than normal (Nelder and Wedderburn 1972). It is applied in various fields due to its flexibility. Simply, the model setting consists of three key components: a distribution, a linear predictor, and a link function. The general formulation of GLMs is:

$$g(E(Y|X)) = X\beta, \quad (11)$$

where Y represents the response variable, chosen from the exponential family (e.g., Binomial, Poisson, or Gaussian). The linear predictor can be expressed as $\eta = X\beta$, where X is the matrix of independent variables, and β is the coefficient vector. The link function $g(\cdot)$ connects the conditional expectation of Y to the linear predictor. Commonly used link functions, depending on the chosen distribution, are the identity, logarithmic and logistic functions.

While the GLMs are powerful and widely used tool for estimation and prediction, they have some limitations. One significant drawback is their assumption of a linear relationship between the predictors and the response variable. When the true relationship is non-linear, the results of GLMs can become biased or yield inaccurate predictions. GAMs address this limitation by extending the GLMs framework to accommodate non-linear relationships (Hastie 2017; Wood 2017). GAMs relax the linearity assumption by replacing linear terms with smooth functions, enabling each predictor to have its own potentially non-linear effect on the response variable. In general, the GAMs take the form:

$$g(E(Y|X)) = \eta = \beta_0 + f_1(X_1) + f_2(X_2) + \dots + f_p(X_p), \quad (12)$$

where β_0 is the intercept term, and $f_j(X_j)$ ($j = 1, \dots, p$) are smooth functions that model the non-linear effects of the predictors X_j on the response variable. The flexibility of GAMs allow them to capture complex relationships while retaining interpretability, making it an effective tool for modeling real-world problems with non-linear dependencies.

A.2 Machine Learning Algorithms

XGB is an advanced implementation of the gradient boosting framework, optimized for performance and computational efficiency (Chen and Guestrin 2016). It is a well-optimized and scalable algorithm that is particularly suitable for regression, classification (binary and multiclass), and ranking problems. The algorithm functions by adding weak learners, such as decision trees, to the ensemble iteratively, with each successive model trying to correct the errors of the previous models. It uses a regularized objective function that includes both the training loss and a penalty term to control model complexity and avoid overfitting. The regularized objective can be written as:

$$\mathcal{L}^{(t)} = \sum_{i=1}^n \ell \left(y_i, \hat{y}_i^{(t-1)} + f_t(x_i) \right) + \Omega(f_t), \quad \text{where} \quad \Omega(f) = \gamma T + \frac{1}{2} \lambda \|\mathbf{w}\|^2. \quad (13)$$

Here, ℓ denotes a differentiable loss function, $\hat{y}_i^{(t-1)}$ is the prediction at iteration $t - 1$, $\Omega(f_t)$ penalizes the complexity of each tree f_t , with T being the number of leaves and \mathbf{w} the vector of leaf weights.

On the other hand, LGBM is a gradient boosting framework designed for speed and efficiency, especially on large-scale data sets with high dimensionality (Ke et al. 2017). It uses Gradient-based One-Side Sampling which selectively retains instances with large gradients to better capture under-fitted samples. Unlike level-wise growth used in other tree-based models, LGBM adopts a leaf-wise tree growth strategy that expands the leaf with the largest loss reduction, which often leads to lower loss with fewer iterations. The model minimizes the following objective function:

$$L(\theta) = \sum_{i=1}^n \ell(y_i, \hat{y}_i) + \sum_{j=1}^K \Omega(f_j), \quad (14)$$

where $L(\theta)$ is the total loss, n is the number of samples, K is the number of trees, and $\Omega(f_j)$ is a regularization term that penalizes the complexity of the model to avoid overfitting.

A.3 Dimensionality Reduction in Modeling

For high dimensional explanatory variables, it is important to be able to reduce the number of variables while preserving valuable information as best possible. Simplifying the data set enhances interpretability, reduces computational complexity, and minimizes redundancy and noise. One widely used method for dimension reduction is principal component analysis. PCA transforms the original variables into a new set of uncorrelated variables called principal components (Hotelling 1933; Pearson 1901). Standardization is needed when the variables in the data set are on different scales.

Given a data matrix X of size $n \times p$ where n represents the number of observations and p is the number of variables, each element in X can be standardized around its mean value, normalized by its standard deviation, thus obtaining a matrix of Z . PCA seeks to find the principal components by calculating the eigenvectors and eigenvalues of the covariance matrix, $\Sigma_{p \times p}$, given by,

$$\Sigma = \frac{1}{n-1} Z^T Z. \quad (15)$$

Singular value decomposition (SDV) is then applied to decompose the covariance matrix, Σ . The eigenvalue equation is expressed as:

$$\Sigma V = \lambda V, \quad (16)$$

where $\lambda_{p \times p}$ is a diagonal matrix consisting of the set of all eigenvalues of Σ along its principal diagonal, and zero for all other elements, and $V_{p \times p}$ is the matrix consisting of all eigenvectors of Σ , one eigenvector per column. The component with the largest eigenvalue becomes the first principal component which explains the greatest variation in the data. The explained variance, σ_{EXP}^2 , by first k eigenvalues is then calculated by:

$$\sigma_{EXP}^2 = \frac{\sum_{j=1}^k \lambda_j}{\sum_{j=1}^p \lambda_j}. \quad (17)$$

The order of the data points in the data set analyzed by PCA has no impact on the results. This is because PCA treats the data set as a collection of vectors and does not account for the sequential or spatial arrangement of the data; the order can be permuted without altering the outcome. This makes PCA unsuitable for analyzing functional data, such as time series or curves, where the sequence of observations holds critical information. Functional principal component analysis extends traditional PCA, tailoring it to analyze data where each observation is a continuous function defined over some domain, rather than a discrete vector (Ramsay and Silverman 2002; Shang 2014).

Let $F(t)$ denote functional data defined over a domain $t \in [a, b]$, where t represents time. Then, functional data can be represented using a basis function expansion, expressed as:

$$F(t) = \sum_{k=1}^{\infty} \beta_k \phi_k(t) + \epsilon(t), \quad (18)$$

where $\phi_k(t)$ are the eigenfunctions (e.g., B-splines, Fourier or monomial basis), β_k are the coefficients associated with each functional principal component, and $\epsilon(t)$ represents noise. Instead of a covariance matrix, FPCA uses a covariance function $C(s, t)$ for decomposition. The eigenfunctions $\phi_k(t)$, and their corresponding eigenvalues λ_k are found by solving the functional eigenvalue problem:

$$\int_a^b C(s, t) \phi_k(t) dt = \lambda_k \phi_k(s). \quad (19)$$

B Tables and Figures

Table B1: Descriptive statistics of each group

		n = 63	Region						
			CEA	CWP	MID	SEA	SPL	SWP	
Group-1	Mean ± SD	504 ± 96	243 ± 72	617 ± 109	1175 ± 109	794 ± 90	888 ± 100		
	Min.	326	84	356	928	526	697		
	Max.	703	427	839	1464	1016	1086		
T90	Mean ± SD	0.40 ± 1.20	0.49 ± 1.31	0.01 ± 0.89	0.54 ± 1.21	0.54 ± 1.42	1.06 ± 1.69		
	Min.	-1.48	-1.65	-1.32	-1.25	-1.61	-1.91		
	Max.	3.57	5.15	3.57	4.49	5.32	5.13		
Group-2	Mean ± SD	3274 ± 275	2727 ± 184	3658 ± 326	1877 ± 236	3346 ± 269	2375 ± 166		
	Min.	2715	2285	3002	1415	2797	2024		
	Max.	3832	3237	4382	2452	4208	2799		
T10	Mean ± SD	-0.46 ± 1.05	-0.15 ± 0.89	-0.30 ± 0.96	-0.44 ± 0.98	-0.28 ± 0.93	-0.31 ± 0.88		
	Min.	-2.11	-1.50	-1.81	-1.84	-1.86	-1.84		
	Max.	1.98	2.42	2.41	2.49	2.88	2.51		
Group-3	Mean ± SD	11.29 ± 2.21	8.31 ± 1.86	10.07 ± 1.73	13.48 ± 2.61	7.02 ± 1.19	3.61 ± 1.04		
	Min.	6.79	3.88	6.10	7.49	4.49	1.54		
	Max.	19.04	13.49	13.82	10.21	10.21	7.02		
P	Mean ± SD	0.10 ± 1.00	0.58 ± 1.16	0.26 ± 1.03	-0.02 ± 0.94	0.33 ± 1.39	0.19 ± 0.97		
	Min.	-2.05	-1.43	-2.13	-2.07	-1.65	-1.92		
	Max.	3.48	2.85	2.95	1.85	5.27	2.93		

Note. n: Number of observations (years), SD: Standard deviation, Min: Minimum, Max: Maximum.

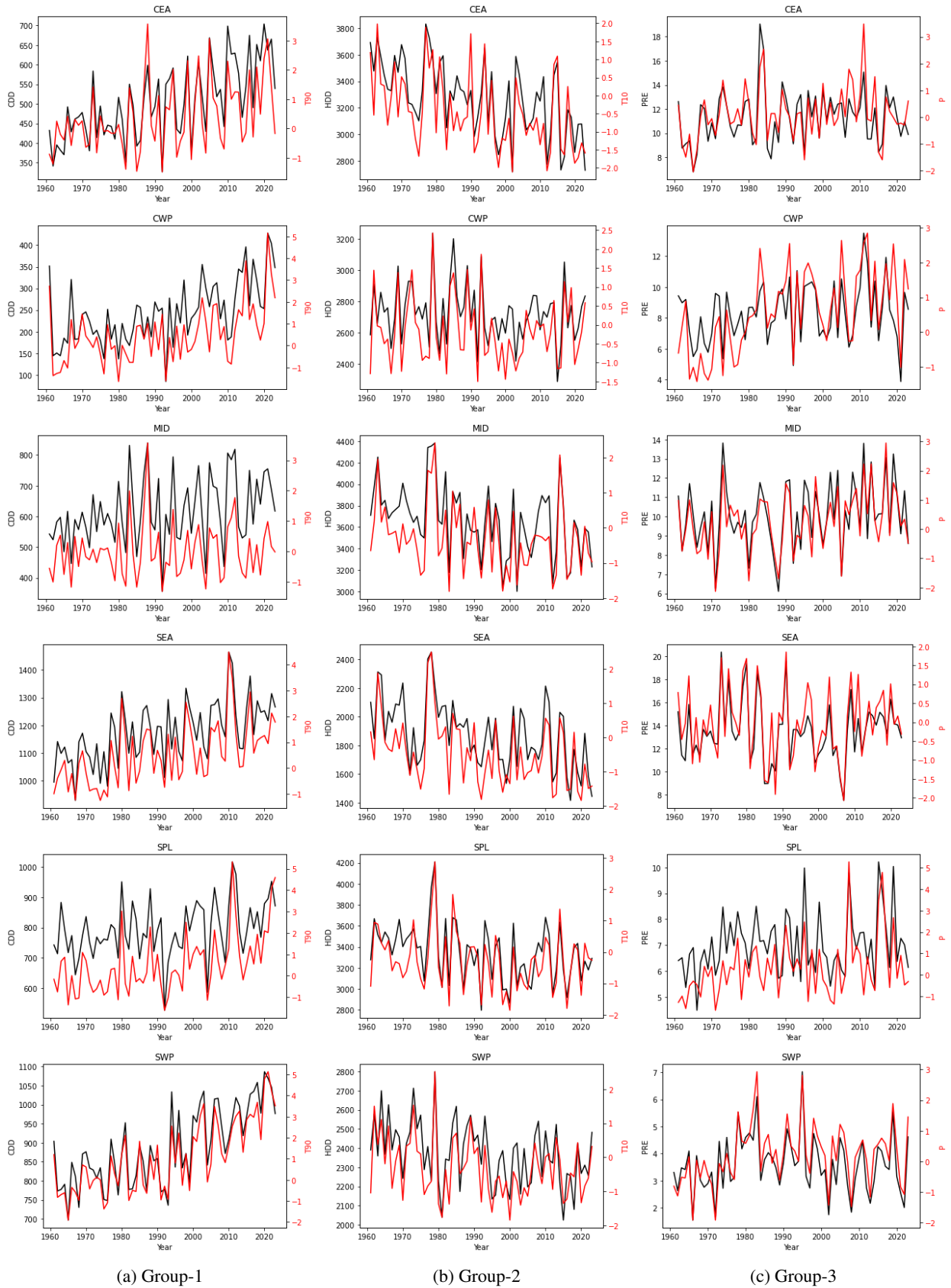


Figure B1: Group indexes of each region over time

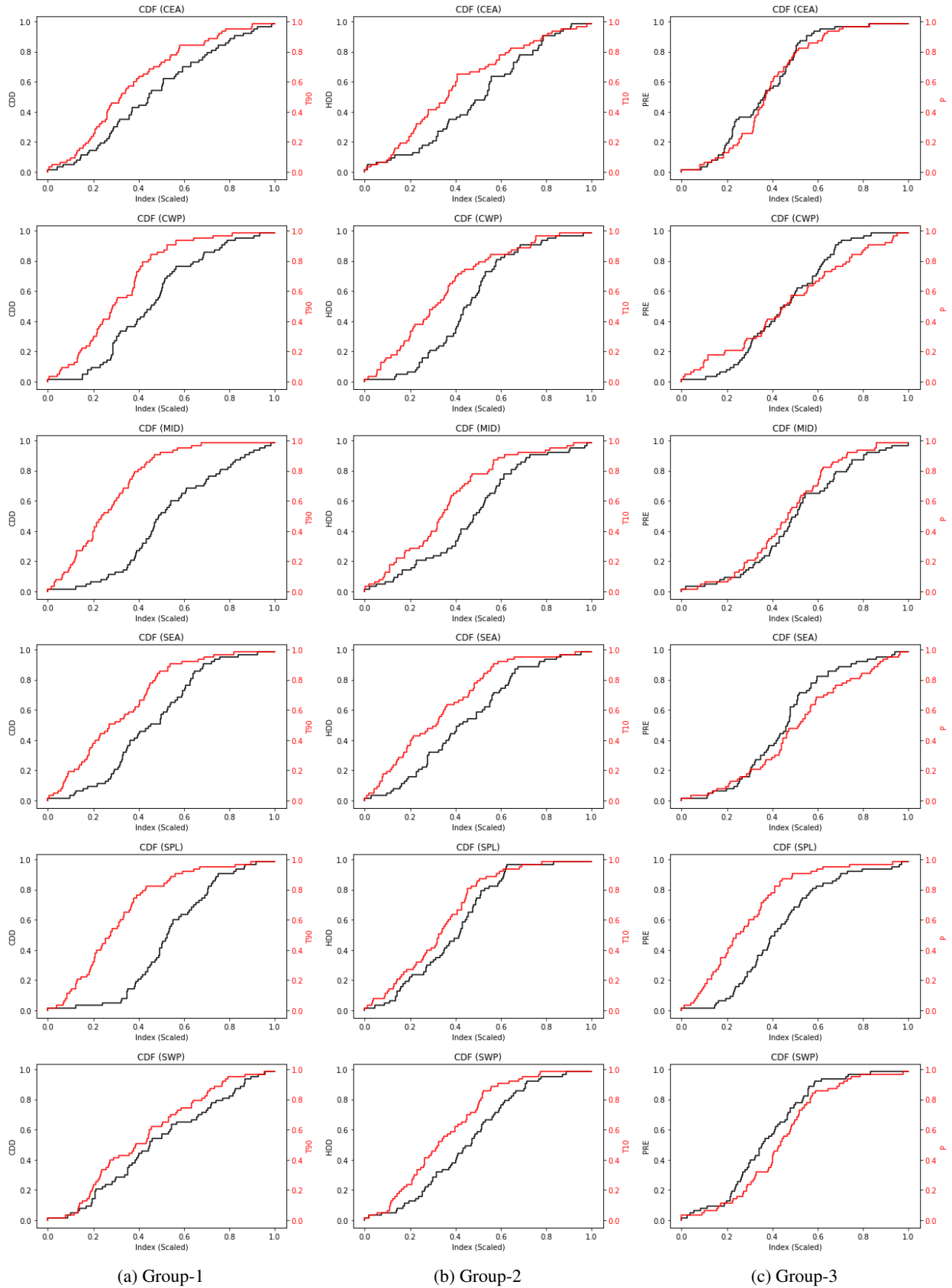


Figure B2: CDF plots of group indexes for each region

Table B2: pR^2 values of GLMs for each crop and region (Train Set)

Crop	Region	Model																					
		1	2	3	4	5	6	7	8	9	10	11	12	13	14	15	16	17	18	19	20	21	22
Corn (Grain)	CEA	0.174	0.276	0.345	0.197	0.493	0.466	0.458	0.122	0.251	0.340	0.347	0.397	0.417	0.374	0.421	0.344	0.632	0.431	0.608	0.608	0.604	0.428
	CWP	0.297	0.292	0.182	0.319	0.240	0.391	0.361	0.313	0.282	0.502	0.322	0.552	0.365	0.593	0.538	0.493	0.452	0.666	0.549	0.504	0.303	0.328
	MID	0.228	0.236	0.249	0.184	0.336	0.291	0.312	0.112	0.101	0.312	0.022	0.322	0.297	0.307	0.338	0.237	0.307	0.292	0.338	0.237	0.292	0.156
	SEA	0.295	0.334	0.113	0.292	0.260	0.280	0.342	0.172	0.214	0.198	0.195	0.185	0.312	0.311	0.231	0.292	0.796	0.220	0.751	0.704	0.687	0.520
	SPL	0.251	0.198	0.105	0.224	0.193	0.212	0.299	0.130	0.128	0.280	0.120	0.286	0.239	0.306	0.337	0.381	0.755	0.386	0.721	0.734	0.736	0.533
	SWP	0.481	0.441	0.026	0.499	0.481	0.479	0.533	0.455	0.412	0.121	0.486	0.489	0.516	0.542	0.487	0.523	0.504	0.524	0.538	0.519	0.466	0.452
Wheat (Winter)	CEA	0.328	0.473	0.065	0.486	0.308	0.440	0.414	0.274	0.444	0.122	0.338	0.334	0.368	0.378	0.484	0.406	0.689	0.478	0.621	0.668	0.674	0.655
	CWP	0.125	0.257	0.216	0.160	0.226	0.390	0.248	0.231	0.270	0.567	0.281	0.661	0.646	0.626	0.581	0.483	0.491	0.487	0.517	0.486	0.290	0.321
	MID	0.202	0.234	0.117	0.284	0.220	0.266	0.281	0.102	0.123	0.159	0.128	0.152	0.190	0.198	0.359	0.262	0.198	0.305	0.359	0.262	0.305	0.174
	SEA	0.295	0.283	0.067	0.271	0.193	0.223	0.242	0.227	0.223	0.111	0.235	0.178	0.111	0.122	0.241	0.117	0.643	0.195	0.606	0.631	0.578	0.570
	SPL	0.281	0.200	0.203	0.277	0.361	0.358	0.387	0.141	0.201	0.308	0.128	0.341	0.377	0.365	0.280	0.324	0.735	0.306	0.774	0.741	0.727	0.528
	SWP	0.341	0.326	0.038	0.330	0.382	0.394	0.423	0.317	0.300	0.167	0.340	0.492	0.404	0.442	0.435	0.403	0.398	0.426	0.433	0.403	0.387	0.384
Soybeans	CEA	0.201	0.328	0.368	0.256	0.542	0.565	0.553	0.167	0.285	0.332	0.375	0.434	0.440	0.430	0.387	0.438	0.614	0.437	0.597	0.624	0.596	0.462
	MID	0.281	0.282	0.255	0.250	0.391	0.362	0.416	0.094	0.152	0.336	0.052	0.346	0.345	0.366	0.389	0.326	0.366	0.344	0.389	0.326	0.344	0.148
	SEA	0.231	0.240	0.248	0.196	0.318	0.395	0.419	0.096	0.149	0.284	0.130	0.193	0.384	0.392	0.285	0.316	0.664	0.259	0.666	0.600	0.572	0.390
	SPL	0.285	0.210	0.146	0.234	0.258	0.227	0.382	0.154	0.145	0.325	0.099	0.390	0.342	0.422	0.387	0.477	0.763	0.457	0.739	0.742	0.753	0.525

Table B3: MAPE values of GLMs for each crop and region (Test Set)

Crop	Region	Model																					
		1	2	3	4	5	6	7	8	9	10	11	12	13	14	15	16	17	18	19	20	21	22
Corn (Grain)	CEA	0.241	0.224	0.288	0.234	0.214	0.204	0.201	0.318	0.225	0.317	0.258	0.309	0.244	0.274	0.211	0.232	0.085	0.176	0.104	0.114	0.134	0.122
	CWP	0.129	0.251	0.351	0.254	0.229	0.314	0.243	0.209	0.277	0.288	0.238	0.244	0.278	0.240	0.243	0.284	0.301	0.164	0.147	0.268	0.226	0.319
	MID	0.281	0.329	0.301	0.321	0.251	0.314	0.255	0.340	0.350	0.305	0.367	0.292	0.304	0.293	0.261	0.275	0.293	0.279	0.261	0.275	0.347	0.279
	SEA	0.168	0.263	0.399	0.269	0.243	0.330	0.238	0.310	0.302	0.339	0.337	0.262	0.227	0.235	0.222	0.246	0.323	0.234	0.347	0.312	0.146	0.321
	SPL	0.159	0.232	0.250	0.244	0.187	0.264	0.184	0.151	0.241	0.248	0.190	0.168	0.235	0.208	0.233	0.181	0.261	0.229	0.168	0.246	0.068	0.291
	SWP	0.176	0.110	0.214	0.124	0.108	0.120	0.051	0.157	0.107	0.225	0.136	0.124	0.102	0.057	0.069	0.102	0.058	0.072	0.049	0.063	0.159	0.077
Wheat (Winter)	CEA	0.174	0.182	0.316	0.162	0.201	0.198	0.176	0.248	0.186	0.307	0.235	0.216	0.235	0.231	0.178	0.211	0.033	0.162	0.045	0.059	0.041	0.146
	CWP	0.218	0.213	0.220	0.181	0.150	0.225	0.181	0.198	0.226	0.140	0.220	0.138	0.154	0.119	0.112	0.174	0.171	0.187	0.170	0.144	0.201	0.161
	MID	0.254	0.290	0.283	0.266	0.242	0.269	0.248	0.317	0.310	0.285	0.325	0.293	0.302	0.291	0.282	0.273	0.291	0.274	0.273	0.282	0.274	0.307
	SEA	0.159	0.220	0.346	0.158	0.233	0.269	0.233	0.247	0.225	0.295	0.269	0.274	0.286	0.276	0.165	0.267	0.106	0.216	0.072	0.081	0.085	0.107
	SPL	0.177	0.212	0.210	0.183	0.155	0.205	0.175	0.146	0.213	0.214	0.172	0.184	0.213	0.195	0.208	0.197	0.127	0.210	0.111	0.110	0.154	0.093
	SWP	0.144	0.114	0.061	0.133	0.073	0.067	0.063	0.167	0.086	0.071	0.124	0.121	0.037	0.073	0.051	0.055	0.107	0.043	0.055	0.068	0.078	0.220
Soybeans	CEA	0.193	0.178	0.255	0.185	0.163	0.153	0.154	0.271	0.179	0.287	0.207	0.264	0.203	0.225	0.187	0.170	0.100	0.143	0.100	0.111	0.107	0.093
	MID	0.232	0.283	0.280	0.273	0.215	0.275	0.223	0.307	0.304	0.279	0.318	0.268	0.266	0.270	0.240	0.239	0.240	0.243	0.270	0.239	0.243	0.308
	SEA	0.231	0.289	0.319	0.294	0.231	0.276	0.238	0.319	0.309	0.285	0.324	0.263	0.218	0.236	0.221	0.244	0.093	0.229	0.060	0.088	0.106	0.216
	SPL	0.184	0.226	0.229	0.221	0.157	0.250	0.175	0.175	0.232	0.231	0.183	0.166	0.212	0.184	0.195	0.153	0.108	0.196	0.114	0.103	0.146	0.129

Table B4: pR^2 values of GAMs for each crop and region (Train Set)

Crop	Region	Model																					
		1	2	3	4	5	6	7	8	9	10	11	12	13	14	15	16	17	18	19	20	21	22
Corn (Grain)	CEA	0.199	0.415	0.345	0.336	0.493	0.528	0.498	0.195	0.650	0.547	0.461	0.596	0.565	0.374	0.623	0.446	0.670	0.473	0.704	0.618	0.712	0.673
	CWP	0.548	0.391	0.452	0.470	0.560	0.391	0.362	0.455	0.480	0.616	0.442	0.673	0.638	0.635	0.619	0.558	0.534	0.681	0.573	0.620	0.435	0.375
	MID	0.228	0.236	0.427	0.215	0.336	0.332	0.490	0.193	0.338	0.442	0.224	0.517	0.616	0.365	0.405	0.482	0.365	0.292	0.482	0.405	0.292	0.156
	SEA	0.328	0.497	0.387	0.516	0.476	0.334	0.412	0.563	0.443	0.334	0.207	0.185	0.493	0.366	0.269	0.591	0.796	0.312	0.729	0.759	0.778	0.693
	SPL	0.393	0.201	0.214	0.281	0.313	0.271	0.299	0.413	0.310	0.345	0.205	0.294	0.426	0.330	0.343	0.465	0.877	0.426	0.893	0.919	0.844	0.703
	SWP	0.612	0.589	0.026	0.558	0.675	0.630	0.602	0.514	0.453	0.212	0.750	0.621	0.580	0.653	0.487	0.653	0.620	0.630	0.756	0.741	0.689	0.497
Wheat (Winter)	CEA	0.468	0.589	0.418	0.608	0.308	0.502	0.496	0.349	0.539	0.465	0.338	0.429	0.634	0.455	0.681	0.583	0.639	0.559	0.705	0.724	0.767	0.677
	CWP	0.475	0.753	0.216	0.621	0.327	0.390	0.478	0.595	0.492	0.635	0.453	0.811	0.700	0.698	0.646	0.559	0.541	0.496	0.498	0.533	0.392	0.349
	MID	0.372	0.411	0.622	0.368	0.351	0.357	0.281	0.279	0.532	0.281	0.252	0.311	0.296	0.364	0.461	0.432	0.461	0.328	0.364	0.432	0.437	0.328
	SEA	0.506	0.423	0.354	0.667	0.287	0.274	0.415	0.451	0.361	0.184	0.360	0.527	0.354	0.272	0.328	0.189	0.667	0.393	0.832	0.652	0.669	0.588
	SPL	0.386	0.453	0.267	0.355	0.579	0.390	0.463	0.396	0.366	0.428	0.315	0.341	0.608	0.375	0.280	0.423	0.800	0.325	0.792	0.757	0.570	0.734
	SWP	0.429	0.459	0.284	0.540	0.382	0.485	0.463	0.317	0.325	0.389	0.438	0.536	0.584	0.583	0.698	0.712	0.487	0.530	0.525	0.463	0.390	0.532
Soybeans	CEA	0.201	0.427	0.387	0.423	0.595	0.644	0.579	0.167	0.608	0.559	0.447	0.643	0.597	0.430	0.545	0.534	0.718	0.453	0.602	0.682	0.652	0.573
	MID	0.323	0.375	0.494	0.250	0.397	0.396	0.548	0.406	0.672	0.360	0.277	0.593	0.620	0.584	0.435	0.616	0.616	0.344	0.435	0.584	0.344	0.423
	SEA	0.358	0.375	0.469	0.465	0.562	0.395	0.488	0.383	0.364	0.443	0.135	0.193	0.559	0.479	0.383	0.728	0.723	0.309	0.685	0.729	0.659	0.472
	SPL	0.426	0.223	0.334	0.272	0.408	0.268	0.520	0.249	0.414	0.362	0.413	0.440	0.507	0.423	0.400	0.580	0.826	0.582	0.842	0.786	0.768	0.642

Table B5: MAPE values of GAMs for each crop and region (Test Set)

Crop	Region	Model																					
		1	2	3	4	5	6	7	8	9	10	11	12	13	14	15	16	17	18	19	20	21	22
Corn (Grain)	CEA	0.228	0.259	0.288	0.289	0.214	0.210	0.185	0.302	0.263	0.303	0.259	0.313	0.255	0.274	0.201	0.289	0.075	0.163	0.102	0.131	0.224	0.108
	CWP	0.294	0.289	0.313	0.400	0.562	0.314	0.243	0.402	0.230	0.305	0.290	0.256	0.261	0.246	0.215	0.288	0.241	0.165	0.172	0.243	0.190	0.302
	MID	0.281	0.329	0.332	0.314	0.251	0.304	0.295	0.359	0.359	0.332	0.389	0.310	0.307	0.305	0.234	0.228	0.305	0.279	0.234	0.228	0.347	0.279
	SEA	0.138	0.248	0.459	0.214	0.254	0.335	0.226	0.295	0.272	0.364	0.330	0.262	0.214	0.228	0.201	0.450	0.323	0.280	0.272	0.183	0.194	0.175
	SPL	0.129	0.230	0.275	0.238	0.156	0.264	0.184	0.170	0.222	0.259	0.171	0.164	0.178	0.196	0.231	0.172	0.085	0.226	0.079	0.167	0.118	0.151
	SWP	0.138	0.104	0.214	0.105	0.159	0.178	0.068	0.097	0.103	0.221	0.260	0.228	0.139	0.155	0.069	0.118	0.118	0.130	0.114	0.228	0.129	0.368
Wheat (Winter)	CEA	0.172	0.197	0.354	0.176	0.200	0.205	0.161	0.235	0.195	0.239	0.235	0.210	0.240	0.239	0.150	0.269	0.042	0.165	0.081	0.088	0.040	0.148
	CWP	0.456	0.207	0.220	0.187	0.168	0.225	0.175	0.165	0.257	0.148	0.240	0.443	0.160	0.117	0.090	0.163	0.168	0.186	0.134	0.170	0.198	0.160
	MID	0.188	0.294	0.293	0.288	0.226	0.265	0.248	0.382	0.286	0.265	0.341	0.320	0.302	0.311	0.281	0.340	0.311	0.282	0.281	0.340	0.282	0.363
	SEA	0.229	0.222	0.399	0.380	0.271	0.275	0.262	0.319	0.204	0.290	0.228	0.305	0.287	0.229	0.150	0.307	0.104	0.225	0.074	0.085	0.066	0.132
	SPL	0.171	0.238	0.217	0.212	0.139	0.199	0.174	0.145	0.175	0.228	0.168	0.184	0.181	0.192	0.208	0.201	0.131	0.215	0.109	0.111	0.151	0.104
	SWP	0.134	0.110	0.109	0.112	0.073	0.069	0.079	0.167	0.086	0.144	0.094	0.125	0.039	0.145	0.067	0.092	0.153	0.044	0.068	0.103	0.161	0.217
Soybeans	CEA	0.193	0.205	0.251	0.235	0.138	0.159	0.140	0.271	0.244	0.257	0.206	0.262	0.205	0.225	0.175	0.224	0.099	0.141	0.097	0.089	0.123	0.155
	MID	0.234	0.290	0.378	0.273	0.214	0.268	0.231	0.314	0.288	0.282	0.345	0.286	0.258	0.278	0.248	0.233	0.233	0.243	0.248	0.278	0.243	0.379
	SEA	0.193	0.279	0.339	0.262	0.221	0.276	0.234	0.294	0.299	0.305	0.324	0.263	0.235	0.240	0.186	0.374	0.093	0.248	0.106	0.107	0.108	0.238
	SPL	0.173	0.221	0.265	0.221	0.211	0.249	0.185	0.169	0.247	0.236	0.230	0.145	0.203	0.184	0.194	0.182	0.077	0.199	0.104	0.108	0.141	0.160

Table B6: pR^2 values of XGB models for each crop and region (Train Set)

Crop	Region	Model																					
		1	2	3	4	5	6	7	8	9	10	11	12	13	14	15	16	17	18	19	20	21	22
Corn (Grain)	CEA	0.673	0.800	0.684	0.726	0.849	0.782	0.738	0.606	0.785	0.753	0.761	0.805	0.771	0.779	0.836	0.760	0.874	0.864	0.861	0.883	0.891	0.811
	CWP	0.795	0.744	0.737	0.817	0.766	0.746	0.717	0.748	0.711	0.835	0.748	0.815	0.854	0.890	0.841	0.844	0.807	0.848	0.841	0.827	0.816	0.728
	MID	0.587	0.670	0.709	0.687	0.705	0.741	0.733	0.630	0.732	0.692	0.500	0.807	0.769	0.703	0.700	0.730	0.703	0.717	0.730	0.700	0.717	0.669
	SEA	0.749	0.794	0.673	0.758	0.746	0.771	0.785	0.656	0.684	0.665	0.707	0.610	0.781	0.800	0.698	0.698	0.761	0.922	0.679	0.899	0.910	0.872
	SPL	0.769	0.677	0.647	0.704	0.617	0.681	0.763	0.627	0.686	0.738	0.647	0.710	0.768	0.732	0.805	0.770	0.941	0.750	0.942	0.954	0.949	0.865
Wheat (Winter)	SWP	0.858	0.800	0.697	0.824	0.857	0.875	0.880	0.871	0.794	0.720	0.885	0.904	0.838	0.931	0.800	0.877	0.903	0.880	0.926	0.910	0.891	0.838
	CEA	0.735	0.790	0.714	0.829	0.705	0.789	0.830	0.737	0.829	0.571	0.729	0.757	0.742	0.751	0.860	0.774	0.909	0.832	0.887	0.898	0.921	0.845
	CWP	0.632	0.804	0.667	0.828	0.762	0.766	0.751	0.718	0.802	0.838	0.732	0.892	0.861	0.893	0.878	0.850	0.841	0.847	0.819	0.824	0.732	0.689
	MID	0.706	0.771	0.685	0.689	0.681	0.696	0.721	0.662	0.645	0.664	0.718	0.698	0.690	0.753	0.721	0.662	0.906	0.790	0.876	0.865	0.850	0.848
	SEA	0.762	0.695	0.598	0.741	0.710	0.677	0.765	0.727	0.651	0.605	0.743	0.714	0.629	0.661	0.722	0.662	0.753	0.721	0.690	0.747	0.747	0.745
Soybeans	SPL	0.734	0.714	0.612	0.697	0.754	0.683	0.763	0.729	0.723	0.713	0.726	0.730	0.687	0.674	0.661	0.712	0.894	0.683	0.895	0.872	0.853	0.807
	SWP	0.779	0.760	0.675	0.731	0.766	0.813	0.827	0.776	0.780	0.755	0.742	0.877	0.827	0.811	0.843	0.872	0.813	0.824	0.865	0.848	0.796	0.796
	CEA	0.685	0.779	0.686	0.733	0.839	0.834	0.815	0.649	0.784	0.727	0.754	0.803	0.822	0.773	0.793	0.720	0.893	0.828	0.883	0.864	0.876	0.810
	MID	0.604	0.707	0.712	0.681	0.745	0.769	0.751	0.664	0.792	0.741	0.563	0.857	0.740	0.754	0.745	0.773	0.754	0.734	0.745	0.773	0.734	0.690
	SEA	0.721	0.731	0.726	0.702	0.809	0.770	0.780	0.714	0.648	0.663	0.679	0.574	0.800	0.805	0.756	0.770	0.914	0.651	0.890	0.867	0.864	0.705
SPL	0.692	0.676	0.700	0.641	0.702	0.718	0.790	0.635	0.682	0.797	0.654	0.726	0.783	0.713	0.786	0.811	0.885	0.795	0.927	0.885	0.880	0.820	

Table B7: MAPE values of XGB models for each crop and region (Test Set)

Crop	Region	Model																					
		1	2	3	4	5	6	7	8	9	10	11	12	13	14	15	16	17	18	19	20	21	22
Corn (Grain)	CEA	0.295	0.251	0.264	0.295	0.166	0.261	0.189	0.326	0.260	0.324	0.267	0.308	0.175	0.301	0.166	0.300	0.119	0.146	0.122	0.194	0.138	0.262
	CWP	0.230	0.269	0.351	0.254	0.279	0.247	0.302	0.318	0.282	0.280	0.369	0.253	0.237	0.236	0.191	0.267	0.234	0.219	0.179	0.237	0.272	0.226
	MID	0.282	0.310	0.367	0.312	0.222	0.301	0.273	0.352	0.329	0.314	0.370	0.264	0.250	0.345	0.301	0.312	0.345	0.244	0.301	0.312	0.244	0.387
	SEA	0.217	0.298	0.419	0.266	0.251	0.369	0.219	0.231	0.269	0.359	0.326	0.284	0.266	0.309	0.217	0.344	0.086	0.314	0.154	0.154	0.145	0.111
	SPL	0.173	0.205	0.282	0.194	0.228	0.270	0.201	0.183	0.215	0.312	0.167	0.154	0.182	0.173	0.225	0.202	0.048	0.208	0.052	0.042	0.057	0.067
Wheat (Winter)	SWP	0.112	0.108	0.243	0.038	0.081	0.130	0.088	0.043	0.114	0.274	0.036	0.079	0.190	0.092	0.077	0.140	0.035	0.073	0.052	0.035	0.076	0.017
	CEA	0.162	0.237	0.329	0.176	0.226	0.249	0.198	0.228	0.211	0.340	0.277	0.257	0.250	0.233	0.171	0.250	0.140	0.179	0.141	0.199	0.141	0.181
	CWP	0.179	0.198	0.177	0.177	0.175	0.182	0.168	0.165	0.245	0.098	0.270	0.110	0.163	0.162	0.128	0.199	0.191	0.157	0.135	0.236	0.222	0.208
	MID	0.206	0.301	0.365	0.280	0.271	0.306	0.279	0.372	0.344	0.278	0.369	0.316	0.284	0.337	0.302	0.351	0.337	0.277	0.302	0.351	0.277	0.371
	SEA	0.249	0.281	0.379	0.292	0.290	0.317	0.193	0.268	0.251	0.321	0.282	0.261	0.286	0.373	0.127	0.300	0.093	0.244	0.180	0.158	0.147	0.170
Soybeans	SPL	0.167	0.236	0.231	0.161	0.178	0.207	0.193	0.182	0.239	0.206	0.220	0.210	0.215	0.185	0.185	0.185	0.065	0.225	0.060	0.068	0.085	0.101
	SWP	0.055	0.102	0.132	0.064	0.075	0.070	0.061	0.092	0.053	0.085	0.071	0.062	0.058	0.104	0.050	0.108	0.087	0.070	0.058	0.091	0.094	0.151
	CEA	0.185	0.230	0.248	0.269	0.156	0.212	0.177	0.286	0.251	0.275	0.226	0.266	0.140	0.264	0.169	0.229	0.123	0.159	0.092	0.142	0.101	0.231
	MID	0.237	0.272	0.314	0.271	0.199	0.271	0.236	0.309	0.261	0.306	0.339	0.236	0.229	0.318	0.273	0.257	0.236	0.236	0.236	0.257	0.318	0.367
	SEA	0.222	0.314	0.330	0.249	0.239	0.315	0.235	0.283	0.264	0.304	0.303	0.304	0.258	0.323	0.198	0.328	0.112	0.299	0.117	0.088	0.087	0.265
SPL	0.209	0.225	0.263	0.199	0.210	0.276	0.174	0.214	0.257	0.265	0.191	0.192	0.196	0.191	0.218	0.185	0.068	0.217	0.085	0.071	0.088	0.132	

Table B8: pR^2 values of LGBM models for each crop and region (Train Set)

Crop	Region	Model																					
		1	2	3	4	5	6	7	8	9	10	11	12	13	14	15	16	17	18	19	20	21	22
Corn (Grain)	CEA	0.206	0.339	0.298	0.307	0.476	0.545	0.416	0.166	0.411	0.335	0.431	0.470	0.497	0.401	0.438	0.427	0.646	0.476	0.619	0.567	0.535	0.316
	CWP	0.442	0.343	0.261	0.405	0.291	0.364	0.370	0.387	0.274	0.519	0.409	0.526	0.530	0.557	0.499	0.592	0.421	0.558	0.608	0.556	0.408	0.315
	MID	0.151	0.252	0.246	0.255	0.338	0.408	0.388	0.121	0.283	0.318	0.119	0.444	0.249	0.236	0.312	0.268	0.236	0.320	0.312	0.268	0.320	0.205
	SEA	0.253	0.239	0.168	0.341	0.285	0.331	0.347	0.113	0.296	0.282	0.158	0.211	0.485	0.379	0.249	0.377	0.658	0.248	0.715	0.671	0.573	0.507
	SPL	0.325	0.192	0.192	0.235	0.190	0.236	0.353	0.240	0.337	0.330	0.172	0.336	0.356	0.373	0.402	0.362	0.797	0.366	0.803	0.707	0.825	0.573
	SWP	0.582	0.492	0.151	0.571	0.516	0.552	0.622	0.553	0.371	0.250	0.599	0.636	0.617	0.619	0.508	0.549	0.666	0.516	0.641	0.719	0.478	0.520
Wheat (Winter)	CEA	0.258	0.489	0.094	0.498	0.335	0.429	0.469	0.354	0.496	0.167	0.308	0.291	0.403	0.354	0.580	0.455	0.618	0.531	0.631	0.709	0.658	0.492
	CWP	0.173	0.349	0.201	0.375	0.320	0.285	0.244	0.433	0.349	0.530	0.408	0.629	0.603	0.576	0.547	0.485	0.549	0.533	0.595	0.572	0.392	0.294
	MID	0.250	0.302	0.148	0.240	0.190	0.195	0.239	0.206	0.177	0.171	0.172	0.175	0.219	0.173	0.353	0.273	0.175	0.390	0.353	0.273	0.390	0.297
	SEA	0.351	0.362	0.135	0.311	0.255	0.258	0.255	0.308	0.278	0.129	0.284	0.236	0.167	0.173	0.323	0.212	0.577	0.216	0.609	0.490	0.488	0.598
	SPL	0.284	0.252	0.245	0.241	0.353	0.321	0.298	0.256	0.283	0.341	0.251	0.328	0.363	0.301	0.309	0.335	0.657	0.253	0.666	0.626	0.607	0.518
	SWP	0.417	0.365	0.152	0.411	0.345	0.437	0.412	0.408	0.324	0.224	0.308	0.545	0.471	0.380	0.392	0.411	0.570	0.522	0.456	0.560	0.506	0.440
Soybeans	CEA	0.226	0.360	0.300	0.323	0.492	0.631	0.494	0.199	0.377	0.311	0.502	0.458	0.516	0.437	0.427	0.435	0.626	0.432	0.630	0.555	0.525	0.370
	MID	0.181	0.281	0.276	0.327	0.394	0.478	0.474	0.114	0.386	0.358	0.162	0.504	0.346	0.276	0.320	0.324	0.320	0.371	0.276	0.324	0.371	0.200
	SEA	0.155	0.137	0.205	0.247	0.303	0.331	0.332	0.060	0.192	0.287	0.092	0.184	0.465	0.318	0.273	0.383	0.604	0.228	0.534	0.543	0.470	0.302
	SPL	0.326	0.229	0.250	0.246	0.239	0.265	0.399	0.209	0.302	0.347	0.183	0.322	0.418	0.385	0.454	0.404	0.684	0.360	0.709	0.617	0.736	0.500

Table B9: MAPE values of LGBM models for each crop and region (Test Set)

Crop	Region	Model																					
		1	2	3	4	5	6	7	8	9	10	11	12	13	14	15	16	17	18	19	20	21	22
Corn (Grain)	CEA	0.301	0.273	0.325	0.260	0.270	0.255	0.255	0.357	0.222	0.325	0.270	0.309	0.233	0.311	0.247	0.273	0.220	0.287	0.213	0.249	0.243	0.254
	CWP	0.246	0.217	0.332	0.267	0.265	0.260	0.264	0.241	0.276	0.277	0.215	0.238	0.207	0.219	0.254	0.312	0.264	0.286	0.197	0.261	0.334	0.281
	MID	0.303	0.320	0.322	0.309	0.253	0.293	0.317	0.330	0.301	0.311	0.336	0.280	0.306	0.332	0.323	0.291	0.332	0.275	0.323	0.291	0.275	0.362
	SEA	0.327	0.352	0.422	0.355	0.341	0.365	0.320	0.402	0.362	0.367	0.363	0.358	0.283	0.305	0.342	0.379	0.256	0.360	0.242	0.231	0.253	0.267
	SPL	0.152	0.216	0.270	0.209	0.172	0.284	0.211	0.168	0.177	0.272	0.194	0.135	0.196	0.172	0.233	0.217	0.080	0.235	0.062	0.101	0.056	0.087
	SWP	0.129	0.155	0.242	0.126	0.139	0.195	0.122	0.049	0.129	0.230	0.054	0.096	0.199	0.086	0.086	0.166	0.166	0.153	0.072	0.045	0.073	0.071
Wheat (Winter)	CEA	0.250	0.216	0.332	0.189	0.234	0.242	0.213	0.246	0.235	0.319	0.250	0.268	0.230	0.244	0.221	0.278	0.194	0.234	0.184	0.202	0.213	0.196
	CWP	0.182	0.215	0.203	0.179	0.201	0.244	0.182	0.187	0.209	0.138	0.237	0.125	0.161	0.132	0.165	0.193	0.173	0.221	0.135	0.239	0.221	0.183
	MID	0.257	0.268	0.300	0.262	0.315	0.287	0.268	0.313	0.302	0.303	0.301	0.306	0.322	0.298	0.291	0.267	0.298	0.247	0.291	0.267	0.247	0.344
	SEA	0.238	0.262	0.356	0.276	0.325	0.261	0.296	0.260	0.265	0.308	0.301	0.304	0.288	0.284	0.234	0.285	0.166	0.267	0.173	0.252	0.222	0.219
	SPL	0.138	0.207	0.237	0.192	0.195	0.228	0.210	0.160	0.210	0.215	0.191	0.186	0.206	0.200	0.165	0.201	0.096	0.198	0.100	0.094	0.098	0.116
	SWP	0.081	0.099	0.066	0.064	0.058	0.053	0.040	0.107	0.075	0.063	0.074	0.048	0.064	0.028	0.030	0.083	0.071	0.079	0.048	0.091	0.110	0.105
Soybeans	CEA	0.263	0.240	0.295	0.227	0.228	0.209	0.216	0.305	0.204	0.290	0.231	0.279	0.201	0.272	0.225	0.252	0.251	0.251	0.187	0.213	0.196	0.213
	MID	0.259	0.289	0.294	0.262	0.214	0.261	0.266	0.308	0.254	0.292	0.299	0.257	0.279	0.293	0.305	0.244	0.233	0.305	0.244	0.293	0.336	0.336
	SEA	0.321	0.323	0.331	0.345	0.286	0.295	0.287	0.385	0.345	0.318	0.342	0.321	0.262	0.300	0.307	0.320	0.247	0.297	0.233	0.241	0.248	0.282
	SPL	0.152	0.210	0.252	0.218	0.195	0.255	0.211	0.175	0.194	0.238	0.212	0.167	0.170	0.178	0.193	0.190	0.094	0.196	0.115	0.134	0.130	0.132

Table B10: pR^2 values of XGB-C models for each crop and region (Train Set)

Crop	Region	Model																					
		1	2	3	4	5	6	7	8	9	10	11	12	13	14	15	16	17	18	19	20	21	22
Corn (Grain)	CEA	0.654	0.673	0.673	0.769	0.843	0.860	0.878	0.678	0.712	0.789	0.802	0.867	0.858	0.884	0.950	0.883	0.958	0.946	0.959	0.962	0.960	0.777
	CWP	0.749	0.708	0.700	0.826	0.847	0.836	0.859	0.817	0.755	0.850	0.860	0.947	0.918	0.957	0.956	0.962	0.956	0.960	0.958	0.962	0.959	0.730
	MID	0.682	0.683	0.750	0.792	0.813	0.826	0.852	0.636	0.743	0.742	0.802	0.841	0.802	0.857	0.927	0.908	0.857	0.931	0.927	0.908	0.931	0.618
	SEA	0.746	0.727	0.675	0.801	0.835	0.831	0.878	0.653	0.702	0.634	0.747	0.823	0.836	0.847	0.907	0.866	0.975	0.934	0.979	0.976	0.978	0.863
	SPL	0.782	0.736	0.617	0.857	0.843	0.811	0.866	0.694	0.682	0.730	0.762	0.875	0.816	0.883	0.913	0.892	0.983	0.920	0.983	0.983	0.984	0.896
Wheat (Winter)	CEA	0.835	0.814	0.560	0.887	0.910	0.885	0.928	0.876	0.774	0.758	0.893	0.925	0.886	0.937	0.946	0.946	0.971	0.955	0.970	0.973	0.974	0.797
	CWP	0.711	0.825	0.546	0.864	0.825	0.863	0.893	0.758	0.811	0.711	0.850	0.831	0.869	0.893	0.942	0.908	0.961	0.952	0.970	0.963	0.971	0.846
	MID	0.659	0.746	0.747	0.792	0.827	0.884	0.901	0.801	0.779	0.878	0.851	0.938	0.930	0.955	0.964	0.958	0.959	0.966	0.967	0.960	0.967	0.782
	SEA	0.662	0.757	0.655	0.774	0.789	0.848	0.859	0.611	0.687	0.605	0.769	0.777	0.790	0.818	0.914	0.824	0.962	0.919	0.961	0.960	0.966	0.803
	SPL	0.763	0.687	0.651	0.800	0.873	0.847	0.887	0.698	0.725	0.744	0.752	0.837	0.846	0.861	0.890	0.883	0.956	0.905	0.961	0.965	0.965	0.832
Soybeans	CEA	0.739	0.760	0.656	0.852	0.874	0.854	0.897	0.747	0.787	0.807	0.846	0.915	0.898	0.929	0.930	0.944	0.966	0.951	0.970	0.967	0.970	0.748
	CWP	0.674	0.730	0.718	0.814	0.831	0.890	0.896	0.696	0.724	0.783	0.812	0.871	0.879	0.905	0.942	0.901	0.961	0.942	0.949	0.952	0.961	0.797
	MID	0.733	0.720	0.738	0.838	0.818	0.865	0.878	0.649	0.798	0.726	0.799	0.863	0.836	0.884	0.927	0.920	0.927	0.946	0.884	0.920	0.946	0.627
	SEA	0.691	0.681	0.744	0.783	0.839	0.829	0.867	0.502	0.717	0.710	0.762	0.772	0.818	0.833	0.922	0.858	0.969	0.938	0.966	0.968	0.971	0.819
	SPL	0.752	0.681	0.693	0.841	0.848	0.851	0.902	0.671	0.684	0.781	0.731	0.872	0.850	0.893	0.917	0.895	0.969	0.915	0.964	0.972	0.976	0.845

Table B11: MAPE values of XGB-C models for each crop and region (Test Set)

Crop	Region	Model																					
		1	2	3	4	5	6	7	8	9	10	11	12	13	14	15	16	17	18	19	20	21	22
Corn (Grain)	CEA	0.247	0.281	0.328	0.280	0.196	0.243	0.206	0.317	0.232	0.373	0.254	0.316	0.249	0.275	0.172	0.285	0.155	0.181	0.150	0.148	0.149	0.237
	CWP	0.217	0.222	0.348	0.222	0.257	0.267	0.244	0.250	0.241	0.281	0.225	0.251	0.256	0.235	0.221	0.240	0.234	0.226	0.232	0.245	0.230	0.304
	MID	0.271	0.329	0.321	0.302	0.301	0.332	0.329	0.382	0.306	0.373	0.313	0.362	0.334	0.308	0.281	0.310	0.308	0.275	0.281	0.310	0.275	0.398
	SEA	0.289	0.269	0.381	0.298	0.293	0.342	0.281	0.347	0.292	0.401	0.291	0.246	0.227	0.192	0.111	0.179	0.051	0.096	0.057	0.056	0.059	0.181
	SPL	0.145	0.261	0.283	0.175	0.164	0.218	0.148	0.218	0.232	0.284	0.195	0.154	0.194	0.150	0.224	0.173	0.049	0.225	0.051	0.055	0.055	0.049
Wheat (Winter)	CEA	0.027	0.100	0.277	0.048	0.031	0.073	0.042	0.045	0.106	0.246	0.032	0.082	0.088	0.076	0.066	0.077	0.049	0.080	0.043	0.049	0.044	0.050
	CWP	0.152	0.172	0.364	0.166	0.170	0.170	0.160	0.268	0.232	0.351	0.244	0.267	0.238	0.236	0.124	0.248	0.156	0.140	0.136	0.145	0.128	0.160
	MID	0.176	0.187	0.201	0.174	0.198	0.186	0.208	0.166	0.162	0.141	0.170	0.152	0.131	0.137	0.113	0.137	0.134	0.120	0.119	0.134	0.117	0.174
	SEA	0.242	0.204	0.350	0.235	0.256	0.236	0.224	0.265	0.238	0.304	0.268	0.203	0.200	0.225	0.121	0.249	0.087	0.112	0.100	0.099	0.101	0.134
	SPL	0.143	0.212	0.226	0.180	0.163	0.207	0.173	0.111	0.221	0.251	0.202	0.171	0.225	0.170	0.181	0.178	0.056	0.163	0.063	0.058	0.064	0.088
Soybeans	CEA	0.069	0.088	0.148	0.091	0.078	0.060	0.077	0.067	0.058	0.067	0.094	0.078	0.044	0.086	0.068	0.070	0.087	0.067	0.082	0.088	0.083	0.071
	CWP	0.199	0.214	0.297	0.217	0.205	0.212	0.187	0.291	0.174	0.331	0.210	0.281	0.225	0.252	0.181	0.251	0.100	0.183	0.100	0.106	0.095	0.199
	MID	0.239	0.292	0.297	0.292	0.255	0.302	0.290	0.343	0.299	0.331	0.305	0.321	0.293	0.279	0.275	0.276	0.279	0.249	0.275	0.276	0.249	0.371
	SEA	0.326	0.337	0.311	0.392	0.255	0.295	0.280	0.375	0.275	0.308	0.243	0.232	0.239	0.202	0.142	0.195	0.088	0.125	0.091	0.093	0.093	0.228
	SPL	0.140	0.259	0.234	0.158	0.172	0.229	0.174	0.166	0.265	0.243	0.185	0.207	0.221	0.201	0.237	0.198	0.068	0.233	0.069	0.086	0.083	0.112